

**A CASE STUDY OF TURBULENT FLUXES DURING A WINTERTIME
PERSISTENT COLD AIR POOL IN THE SALT LAKE VALLEY**

by

Jai Kiran Sriramasamudram

A thesis submitted to the faculty of
The University of Utah
in partial fulfillment of the requirements for the degree of

MASTER OF SCIENCE

Department of Mechanical Engineering

The University of Utah

August 2009

Copyright © Jai Kiran Sriramasamudram 2009

All Rights Reserved

ABSTRACT

Local turbulence processes during the formation, maintenance and destruction of persistent cold air pools are relatively unknown. A wide variety of mechanisms are involved in the formation and destruction of persistent cold air pool that contribute to this problem. In this work, two persistent cold air pool episodes were observed during February 2004 in the Salt Lake valley. The two inversion episodes were separated by a brief 'washout' period when the persistent cold air pool was destroyed. The current research presents near surface turbulence measurements including fluxes of heat, momentum and water vapor during February 2004 from a measurement site located at the south-west end of the Salt Lake valley. The turbulence levels during the persistent cold air pool episodes compared to turbulence during a period that was not under the influence of a cold air pool were reduced by over 70%. Meteorological data from various regional weather monitoring stations has been utilized to conjecture two types of mixing scenarios during a persistent cold air pool namely: a surface based inversion scenario and a well mixed surface layer capped by an elevated inversion. It is shown that both of these types of cold air pools can exist during a single persistent cold air pool episode

TABLE OF CONTENTS

ABSTRACT	iv
LIST OF FIGURES.....	vi
CHAPTERS	
1. INTRODUCTION	1
1.1 Background	1
1.2 Literature Review	5
1.3 Scope of Current Research	12
2. SITE AND INSTRUMENTATION	14
3. VALLEY METEOROLOGY	40
4. LOCAL TURBULENCE	40
3.1 Monthly Average	40
3.2 Warm Air Advection	44
3.3 Cold Pool/Non Cold Pool Comparison	48
5. CONCLUSIONS	57
APPENDIX	59
REFERENCES	79

LIST OF FIGURES

1.1 Schematic representation of formation and destruction of diurnal CAP	3
1.2 Schematic representation of different phases during a persistent CAP	4
2.1 A CSAT3 Sonic Anemometer coordinate system and mounting hardware (courtesy. Campbell Scientific. Inc.).....	15
2.2 Location of the Kennecott site	17
2.3 Instrumentation at the Kennecott site. The sonic anemometers point 190°	18
3.1 Surface weather maps at 0500 LST from 11 through 15 February 2004.....	20
3.2 24 hour average of precipitation from 11 through 15 February 2004.....	21
3.3 Hourly average of cloud height and type from 10 through 29 February 2004	22
3.4 Hourly average of visibility from 11 through 29 February 2004	23
3.5 Topographic map of the Salt Lake valley showing the mesowest stations	26
3.6 Hourly average of temperature from SLC Airport, Baccus and Empires Peak and SLC Airport sounding at 0500 LST and 1700LST from 11 through 15 February 2004.....	27
3.7 Surface weather maps at 0500 LST from 16 through 19 February 2004.....	29
3.8 24 hour average of precipitation from 11 through 15 February 2004	30
3.9 4 hour average of temperature, relative humidity, wind speed and wind direction from 11 through 28 February 2004	31
3.10 Hourly average of temperature from SLC Airport, Baccus and Empires Peak and SLC Airport sounding at 0500 LST and 1700LST from 16 through 19 February 2004 ...	32
3.11 Surface weather maps at 0500 LST from 20 through 24 February 2004.....	35
3.12 24 hour average of precipitation from 20 through 24 February 2004.....	36

3.13 Hourly average of temperature from SLC Airport, Baccus and Empires Peak and SLC Airport sounding at 0500 LST and 1700LST from 20 through 24 February 2004 ...	37
3.14 Two types of cold air pool mixing scenerios	38
3.14 Type 1 and Type 2 scenario from 11 through 28 February 2004	39
4.1 30 minute and daily averages of wind velocity, temperature, sensible heat flux, turbulent shear stress and kinetic energy from 11 through 29 February 2004.....	41
4.2 Hourly average of temperature, wind speed and wind direction at Kennecott from 16 through 19 February 2004.....	45
4.3 Hourly average of temperature, wind speed and wind direction at Bluffdale from 16 through 19 February 2004.....	45
4.4 30 minute average of sensible heat flux at Kennecott from 17 through 18 February 2004.....	46
4.5 30 minute average of Turbulent Kinetic Energy at Kennecott from 17 through 18 February 2004	47
4.6 30 minute average of Turbulent Shear Stress at Kennecott from 17 through 18 February 2004	47
4.7 5 day ensemble average of mean temperature measured at 9.16 m AGL at Kennecott for February and March 2004	49
4.8 5 day ensemble average of normalized mean temperature measured at 9.16 m AGL at Kennecott for February and March 2004.....	49
4.9 Shear stress averaged from 11 through 15 February 2004 and compared to shear stress averaged from 11 through 15 March 2004 at Kennecott	50
4.10 Sensible heat flux averaged from 11 through 15 February 2004 and compared to sensible heat flux averaged from 11 through 15 March 2004 at Kennecott	52
4.11 Latent heat flux averaged from 11 through 15 February 2004 and compared to latent heat flux averaged from 11 through 15 March 2004 at Kennecott	52
4.12 TKE averaged from 11 through 15 February 2004 and compared to TKE averaged from 11 through 15 March 2004 at Kennecott.....	54

4.13 Friction velocity averaged from 11 through 15 February 2004 and compared to friction velocity averaged from 11 through 15 March 2004 at Kennecott54

4.14 Wind speed averaged from 11 through 15 February 2004 and compared to wind speed averaged from 11 through 15 March 2004 at Kennecott56

4.15 Wind direction averaged from 11 through 15 February 2004 and compared to wind direction averaged from 11 through 15 March 2004 at Kennecott56

CHAPTER 1

INTRODUCTION

1.1 Background

A number of large cities such as Salt Lake City (UT), Phoenix (AZ), Los Angeles (CA), Las Vegas (NV), and Denver (CO) are located amongst complex intermountain terrain. One of the major features of basins and valleys is the formation of a *cold air pool* (CAP). A Cold air pool, by definition is a ‘topographically confined, stagnant stably stratified layer of air that is colder than the air above’ (Whiteman et al. 2001). Cold air pools can be categorized into two types based on their persistence over a period of time; diurnal cold air pools and persistent cold air pools. Diurnal CAPs are formed due to long wave radiation loss from the Earth at night during the absence of incoming solar radiation. As a result, the surface cools down with air above being warmer than the surface. This leads to a negative sensible heat flux, meaning the heat flux is directed from the atmosphere toward the surface of the earth and this process takes place through the course of the night leading to growth in the stable boundary layer (Stull, 1988). Diurnal CAPs form as a result of accumulation of cold air at the surface of the valley over the night due to the initiation of down slope winds. The down slope winds along the slope of the valley are initiated due to the air near the slope being denser than the air parcel not

adjacent to the slope at the same elevation (Whiteman, 1990). This is illustrated in Figure 1.1a. The depth and strength of diurnal cold air pools depend largely upon the surrounding terrain and synoptic weather situation (Whiteman et al. 2001). They are typically eroded and destroyed during the daytime as the convective boundary layer begins to grow which is illustrated in Figure 1.1b.

Persistent CAPs which typically form during the winter, unlike diurnal CAPs, last for several days as the daytime sensible heating is not sufficient to break the inversion. Figure 1.2 illustrates one of the various mechanisms in which a persistent CAP forms and is destroyed. A persistent CAP may form as the result of a nocturnal inversion on a clear night. The inversion initially nocturnal in nature may transition into a persistent CAP due to the advection of warm air above producing a sharp stable layer at the top of the CAP. The presence of stratus clouds may exacerbate the situation by inhibiting the penetration of sunlight into the basin, preventing the convective boundary layer from growing and destroying the inversion within the basin. Persistent CAP episodes are often destroyed with cold air advection aloft destabilizing the basin atmosphere and breaking the stratus deck allowing sunlight to penetrate and destroy the inversion with the upward growth of a convective boundary layer from the heated surface.

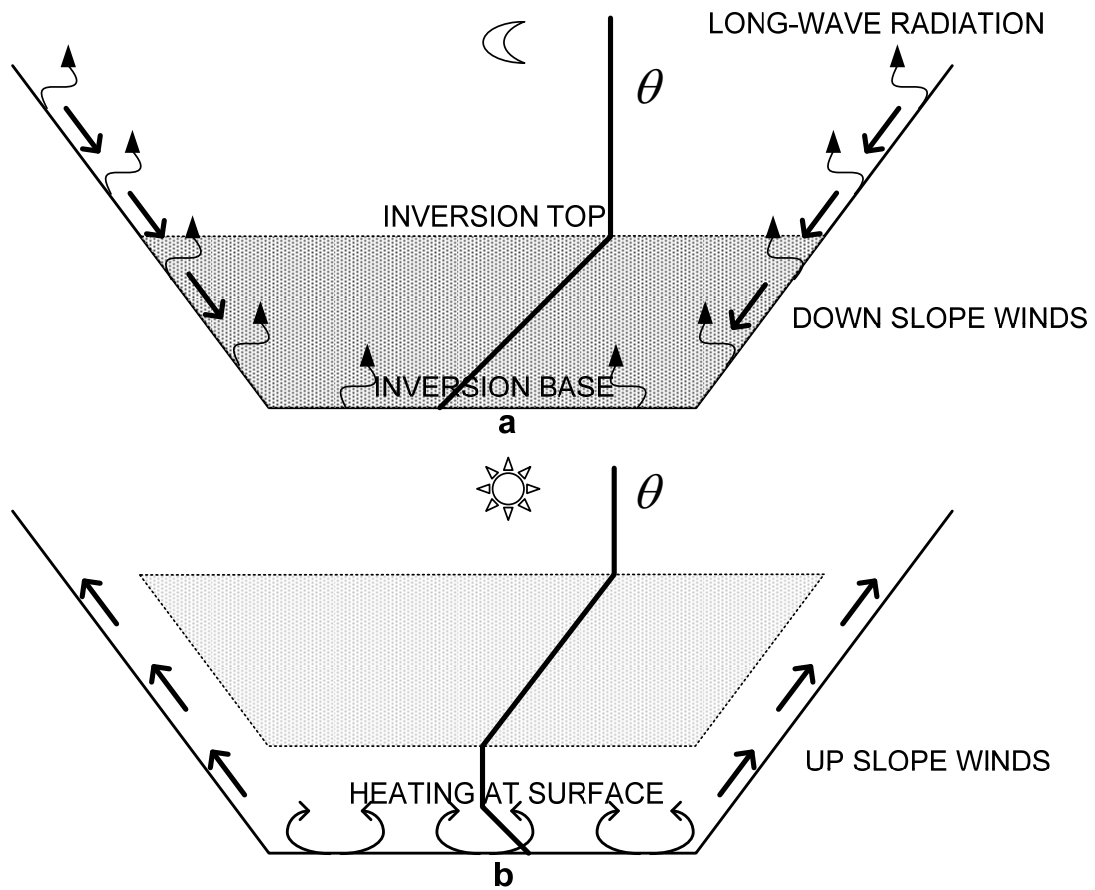


Figure 1.1 Schematic representation of formation and destruction of a diurnal CAP.

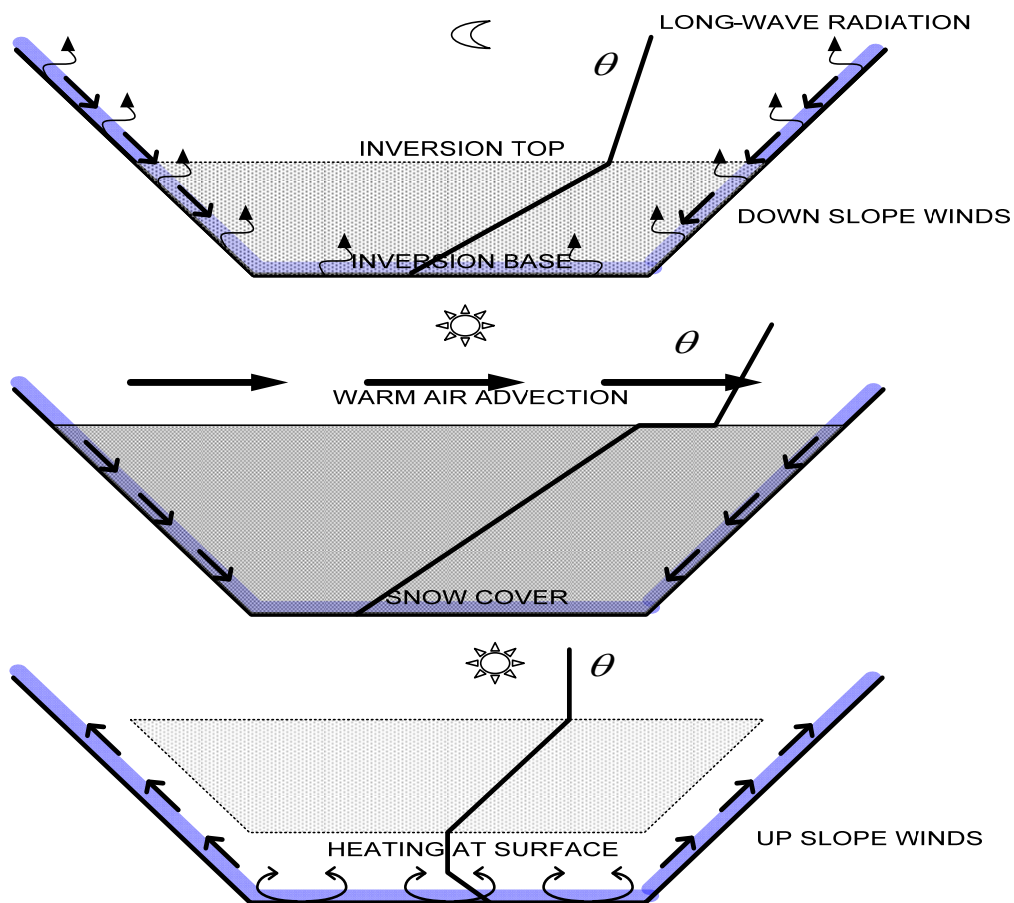


Figure 1.2 Schematic representation of different phases during a persistent CAP.

Why is understanding the nature of cold air pools important? With increasing human population in basins and valleys and with the presence major power plants and heavy industries, industrial and vehicular emissions released during a CAP episode undergo little dispersion resulting in buildup of pollutant concentrations. Human activities and transportation are disrupted during CAPs because an event is often accompanied by periods of low clouds and fog. Huge buildup of pollutant concentrations were recorded during wintertime CAPs in Denver, Colorado (Reddy et al. 1995). Air pollution episodes in Slovenia and Croatia have been studied and models have been developed (Petkovsek et al. 1978, 1980, 1992). In the Lake Powell area of Utah, stagnant

conditions associated with slow-moving high pressure systems were found to dominate the climate during winter. The worst air quality was observed when a stagnation episode was accompanied with snow cover on the ground and/or when the sun angle is low (Yu and Pielke et al. 1986). The mixing volume, product of mean wind speed and the height of convective boundary layer, when multiplied by time and length perpendicular to the wind provides an estimate of the volume of air in which the pollutants are mixed. This mixing volume was consistently found to be very low during a persistent CAP episode (Wolyn and McKee et al. 1989). Persistent CAP episodes characterized by low clouds and fog were investigated in the central valley of California (Holets and Swanson et al. 1981, Lockhart et al. 1943). Besides poor air quality, ground transportation is often compromised by cold air pools. In Alaska, ground transportation is interrupted by thawing snow and ice interfering under cool climatic conditions (Smith et al. 1997). “Hazardous and destructive episodes of freezing rain” are known to occur during cold pools (Smith et al. 1997). Understanding the fundamental nature of CAPs is not only essential to forecast such an event but also to site new businesses, industries and transportation facilities (Smith et al. 1997).

1.2 Literature Review

In the winter of 1998-1999 two persistent cold pool episodes, (24 -26 Dec 1998, 2-7 Jan 1999), were investigated (Whiteman et al. 2001) to gain an understanding of the various processes responsible for the build-up, maintenance and break-up of persistent wintertime cold pools. The cold pool episodes took place in the Columbia basin of eastern Washington and Oregon - a basin located between the Cascade and Rocky

mountains. The first cold pool episode was initiated 19 December when an arctic cold front approached the basin and continued through 23 December when the basin was filled with cold air. A low pressure system approached the Pacific north-west coast causing a warm front to move northward along the Oregon coast on the afternoon of 24 December with warm air advected over the Columbia basin. The cold pool was eventually destroyed when a strong lee wave caused the warm air to descend along the slopes, progressively replacing the cold air in the basin. The second cold pool episode formed as fog and clouds developed within a nocturnal temperature inversion at the end of a clear night. A stable layer formed with the synoptic-scale advection of warm air. Fog and clouds prevented sunlight from penetrating into the basin and destroying the cold pool by the growth of a convective boundary layer. The cold pool began to strengthen as the strong stability cap at the top of the pool descended into the basin. The cold pool was destroyed when a cold front destabilized the basin atmosphere with penetration of sunlight causing the convective boundary layer to grow.

For the persistent cold pool episode that took place on 2 -7 January 1990, Regional Atmospheric Modeling System (RAMS), a three dimensional, non-hydrostatic, mesoscale numerical model, was used to evaluate the relative importance of different physical mechanisms in the formation, maintenance, and destruction of the persistent cold air pool (Zhong et al. 2001). The simulation showed that the cold pool formed as a result of cold air being trapped due to a strong capping inversion produced as a result of strong westerly winds descending in the lee of the Cascade Mountains. Fog and stratus prevented sunlight from reaching the basin floor. The role of fog, a common feature of wintertime cold pools did not play a major role in maintaining the cold pool episode since

the solar heating during midwinter is often insufficient to destroy the persistent cold pool episode even during the absence of low-level clouds. The role of low-level clouds becomes critical in the spring as they can inhibit the sunlight from reaching the basin floor to destroy the cold pool. The destruction of the cold pool was accomplished by cold air advection aloft coupled with surface heating and turbulent mixing. The turbulent erosion which is responsible for removing the cold air from the top of the pool did not prove to be critical, as the turbulence produced due to shear between the weak winds within the pool and strong winds aloft was balanced by negatively buoyant air produced by temperature jump at the top of the pool. While the RAMS simulations of Zhong et al. (2001) captured several features of the cold pool episode, it failed to produce some of the details of evolution of temperature structure observed during the event. Uncertainty in the prescribed soil moisture values, which is responsible for temperature evolution and formation of fog and low level clouds was one of the major limitations in using the model for the study.

In another study, Wolyn and McKee (1989) studied the development of deep stable layers (DSL) at Salt Lake City UT, Boise ID, Winnemucca NV and Grand Junction CO. They concluded that if 65% of the lowest 1.5km of the 0500 MST sounding has a lapse rate of $2.5^{\circ}\text{C}/\text{km}$ or less then the day was under the influence of a deep stable layer or a cold pool. A cold pool episode in December 1980 was examined to gain an understanding of the life cycle of the cold pool. It was observed that a persistent wintertime cold pool episode was initiated when a layer of warm air decoupled the already-present cold air from the upper atmosphere, preventing the daytime convective boundary layer from mixing and growing. The presence of barriers also restricted the

horizontal movement of the cold air near the surface. The presence of a capping stable layer helped prolong the cold pool episode. Presence of fog for the entire day can also help in prolonging the episode due to high albedo and long-wave cooling. The termination of a cold pool episode was due to the weakening of the synoptic scale ridge aloft with associated cooling.

Wintertime temperature inversions in the basin of the Colorado plateau were investigated over a period of three months- 10 Jan 1990 through 31 March 1990 by Whiteman et al. (1999). The Colorado Plateau covers an area of about 225,000 Km² in western Colorado, north-western New Mexico, eastern Utah and northern Arizona and is well known for persistent potential temperature inversions in winter. This study was focused on determining the characteristics of wintertime inversions in the Colorado Plateau basin, and investigating the physical processes responsible for their formation, maintenance and destruction. Due to the low frequency of the soundings made during the study, the data was primarily used to focus on the bulk characteristics of the inversion in the basin and not rapid evolutionary changes which take place during the diurnal buildup and breakup. Two different analytical approaches were followed to investigate the buildup, maintenance and breakup of the basin inversion. The first approach used the relative changes in potential temperature measured on the basin floor and top to monitor the buildup, maintenance and decay, while the second approach used the basin heat deficit computed from deviations of potential temperature in the basin relative to that at the top, weighted by basin volume at various altitude intervals. The study concluded that the buildup usually takes place over a multi-day period when a synoptic scale event such as warm air advection aloft occurs in advance of approaching synoptic scale ridges. Once

an inversion has formed, it can last for several days as the daily heating is weak and cannot provide the thermal energy required to overcome the basin heat deficit. The stable atmosphere in the basin protects it from the strong overlying winds causing the winds at lower elevations to be weak and variable in direction. During mid winter the inversion begins to decay rapidly when cold air advects in advance of approaching synoptic scale troughs. This cold air advection, however, was found to be insufficient to destroy the inversion in the basin. By the end of February, the basin heat deficit decreases and the convective boundary layers grow deeper, breaking the inversion on a daily basis. Through this study the mean potential temperature gradients within the basin inversion were determined to be less than isothermal (0.0098K/m) and thus a true temperature inversion was absent. Since the wintertime inversion in the Colorado Plateau basin did not have a distinctive high stability top that separated the basin from the free atmosphere the use of the term 'cold air pool' to represent the wintertime inversions was avoided. The basin atmosphere was affected mostly by synoptic scale flows with relatively weak potential temperature gradients indicating the inability of the confining topography to protect the basin atmosphere from the influence of synoptic scale flow.

A mesoscale numerical model was developed by Lee et al. (1989) to examine the influence of a CAP downstream of (1) a symmetric bell shaped mountain and (2) an asymmetric mountain on the generation of downslope wind storms along with the importance of orientation of the synoptic surface pressure pattern. The phase and amplitude of linear and nonlinear hydrostatic mountain waves was accurately predicted by the model. It was observed that the presence of a CAP downstream of the mountain greatly influenced the mountain wave structure near the surface and above. The

simulation of the model showed that the top of the cold pool resembled the shape of the terrain. Winds on the lee slope of the mountain were limited to downslope propagation. The presence of the CAP inhibited the strong downslope winds from reaching the surface. In other words, until the cold air was flushed out, the downslope winds could not reach the surface. It was concluded that in the absence of surface heating, a strong geostrophic wind directed away from the mountain barrier must be present in order to advect the strong cold pool away from the terrain and allow the downslope winds to reach lower elevations on the lee slope of the mountain. It was also observed that the orientation of the synoptic-scale pressure gradient was more efficient in flushing the cold pool when compared to the effect of forced mountain wave near the surface. Turbulent mixing at the top of the cold pool, as in other studies, was found to be insignificant in destroying the cold pool.

Vrhovec et al (1991) developed a meso-meteorological model which was used to study the formation of CAPs. The model was used to simulate adiabatic flow around an isolated mountain, adiabatic channeling through a valley in between two mountains and nocturnal wind circulations in a small elongated basin. For the first two cases, with the basin atmosphere stably stratified, the model produced blocking with most of the wind flowing around the obstacle and with vertical components small in magnitude. For the second case, the model produced strong channeling between the two mountains and two vortices on the lee side of the two mountains. For the third case, the wind pattern produced by the model displayed the growth of the cold pool within the basin. Downslope winds were produced as a result of radiative cooling. Finally, the model was used to simulate the nocturnal wind pattern in the Slovenj Gradec basin, an alpine basin

in northern Slovenia. The model showed that a cold air pool forms three hours after radiative cooling begins at the surface. A downvalley wind system is initiated as a result of radiative cooling, filling the basin with cold air. Once the cold air pool formed, winds within the cold pool became weak while strong winds continued above the inversion top. The basin atmosphere became decoupled from the atmosphere above. The wind pattern in the basin was not related to that at the top.

In late December 1999 Johnson et al (2000) performed an investigation to understand the mechanisms responsible for the evolution, maintenance and decay of a persistent cold pool in the Helena valley in Montana surrounded by the Elkhorn Mountains on the south, the Rocky Mountains on the west and the Big Belt Mountains to the north and east. The study focused on using synoptic model guidance. The cold pool was initiated with the passage of an arctic front over the valley, followed by an upper level ridge. The cold pool developed on the night of 23 December and did not break until afternoon of next day. The cold pool which was thought to be diurnal in nature transitioned into a persistent cold air pool. The cold pool strengthened each day as the temperatures in the valley decreased and as daytime heating was insufficient to destroy the cold pool. The cold pool was finally destroyed on the afternoon of 29 December when the upper level ridge began to break with the passage of cold air aloft, causing the cold air pool to dissipate. It is pointed out that throughout the study the use of NGM and AVN MOS proved highly ineffective in their temperature forecasts for the onset, continuation and destruction of the persistent cold air pool.

1.3 Scope of the Current Research

Formation of persistent CAPs in valley and basins in many parts of the world are well documented, as discussed in the previous section. Forecasting the buildup and breakdown of persistent CAPs is important, as there are high population densities in valleys and basins. The extreme variation of atmospheric processes that affect the evolution and decay of persistent CAPs pose a serious challenge in conducting theoretical and observational studies (Smith et al. 1997). The lack of frequent vertical soundings and logistic problems encountered in running wintertime studies are among many other reasons that have hampered our understanding of processes affecting the persistent CAPs (Whiteman et al. 2001). Much research has focused on persistent CAPs using remote sensing instruments. Improved model formulations have been directed to determining the fundamental mechanisms that are responsible for the formation, maintenance and destruction of persistent CAPs in various parts of the world. However, very little work has been focused on quantifying small scale processes of turbulence during persistent CAP episodes. The research performed in this work has investigated a number of research questions associated with CAPs in the Salt Lake Valley including, What is the magnitude of turbulence during a persistent CAP episode?, what is the temporal variation of different turbulent variables such as momentum flux, turbulent kinetic energy, fluxes of heat, momentum and water vapor during the formation, maintenance and breakup, and how does the variation of the above mentioned variables in a cold pool compare to those during a non-cold pool period? Two persistent CAP episodes were observed during February 2004. The first episode began on 11 February 2004 and lasted until 15 February 2004. The second episode began on 20 February 2004 after the destruction of the first

episode. The second episode lasted until 24 February 2004. During this period turbulent fluxes of sensible heat, momentum and water vapor along with turbulent kinetic energy and near surface turbulent momentum flux were measured. These quantities are discussed during the evolution, maintenance and erosion of a persistent CAP. The data are then compared to a period with similar solar forcing (i.e. same time of the year) but not under the influence of a persistent cold air pool. Chapter 2 describes the measurement sites and instrumentation. Chapter 3 discusses the weather in the Salt Lake valley during February 2004 by analyzing surface weather maps. Also utilized are time series of meteorological variables such as temperature, humidity, wind speed and direction from several weather monitoring stations in the valley along with twice-daily rawinsonde soundings from Salt Lake City International Airport. The three sections in Chapter 4 present; (a) daily average of turbulent variables such as sensible heat flux, wind shear, and turbulent kinetic energy for February 2004, (b) timing of the warm front that separated the two cold pool episodes and that was responsible for modifying the valley weather during that period, and (c) comparison of the behavior of the above mentioned turbulent variables during the first inversion episode with a similar wintertime period which was not under the influence of a persistent CAP.

CHAPTER 2

SITE AND INSTRUMENTATION

Measurements for the current project were made at the Kennecott site on the south-west end of the Salt Lake valley at the foot of Ocquirh Mountains and right next to the intersection of Hwy U-111 and 11800 South (Figure2.2). Coordinates of the Kennecott site are 40.5551°N and 112.0703°W . The Kennecott site is a pre-urban neighborhood located 1585 m above sea level. This pre-urban site is characterized by shrubs and grass measuring up to 0.5 m. A fallow agricultural field is situated north and northwest of the site. The Trans Jordan landfill is located approximately 1km to the northeast of the Kennecott site. The Kennecott Copper Mine is southwest of the site. Since the site is located at the foot of the Ocquirh Mountains, winds are observed to flow upslope (anabatic) during the daytime owing to density variations in and above the growing convective boundary layer. During nighttime, the upper atmosphere cools down due to radiation loss and the air parcels just above the mountain slopes become denser than the air parcels situated at the same elevation away from the slopes causing the air parcels just above the slopes to flow down slope (katabatic).

The Kennecott site was equipped with three Campbell Scientific CSAT3 sonic anemometers which measure temperature and wind velocities in axial, longitudinal and vertical directions at a frequency of 10 Hz. The sonic anemometers were mounted on a 7

m tower constructed over a platform measuring 2 m above ground level. The sonic anemometers were mounted at 5 m, 7 m and 9 m above ground level as shown in Figure 2.3. A sonic anemometer consists of 3 pairs of piezoelectric transducers aligned on three non-orthogonal axes. Each transducer behaves as a transmitter as well as a receiver. An acoustic signal is sent simultaneously in opposite directions between the transducers. Wind velocity is determined by measuring the difference in transit times of the acoustic pulses. Accuracy of CSAT3 sonic anemometers measuring wind velocities is $\pm 4 \text{ cm s}^{-1}$ and the operating temperature range is -30°C to 50°C . A schematic of a CSAT3 sonic anemometer is shown below.

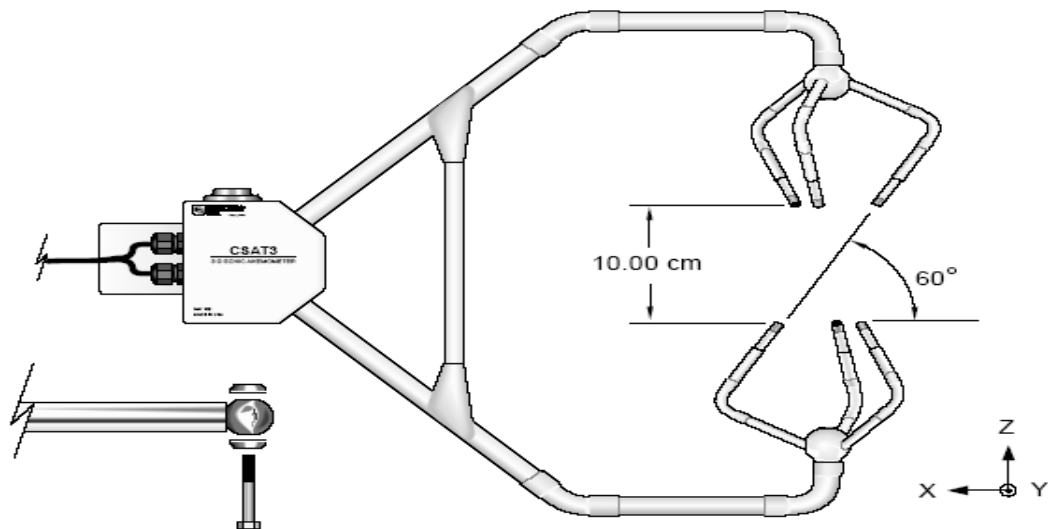


Figure 2.1 A CSAT3 Sonic Anemometer coordinate system and mounting hardware (courtesy, Campbell Scientific Inc.)

A LICOR 7000 Infra Red Gas Analyzer (IRGA) was used to measure carbon dioxide concentration in micromoles per mole and water vapor concentration in millimoles per mole. The ambient air sample is transported into the IRGA using a 7 m long tubing with a diameter of 0.25 inches. The air sample passes through a gelman filter where the particulate matter is filtered. The carbon-dioxide and water vapor measurements are based on the difference in absorption of infrared passing through two gas sampling cells. The reference cell or cell A contains known carbon dioxide or water vapor concentration. The sample cell or cell B contains unknown concentration of carbon-dioxide or water vapor. Infrared radiation is transmitted through both cell paths and the radiation at the detectors is measured in both cells and used to compute absorption. A Neuberger pump was used to suck the air through the 7 m long tubing situated at 9 m above ground level close to the center of the sonic paths. A laminar flow ($Re=375$) was maintained in the tubing with a flow rate of approximately 1.5 liters/minute. The 10 Hz data from the three CSAT3's and LI-7000 is streamed into a Campbell Scientific CR5000 datalogger. The data streamed into the datalogger is stored onto a memory card. The data from the memory card is later transferred to a secure server.

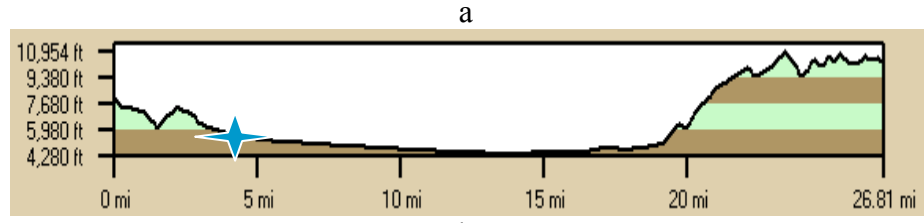


Figure 2.2 Location of the Kennecott site (a) indicated by the red circle in the topographic map of Salt Lake Valley. (b) indicated by the star in the elevation profile along the east-west transect shown in the topographic map.

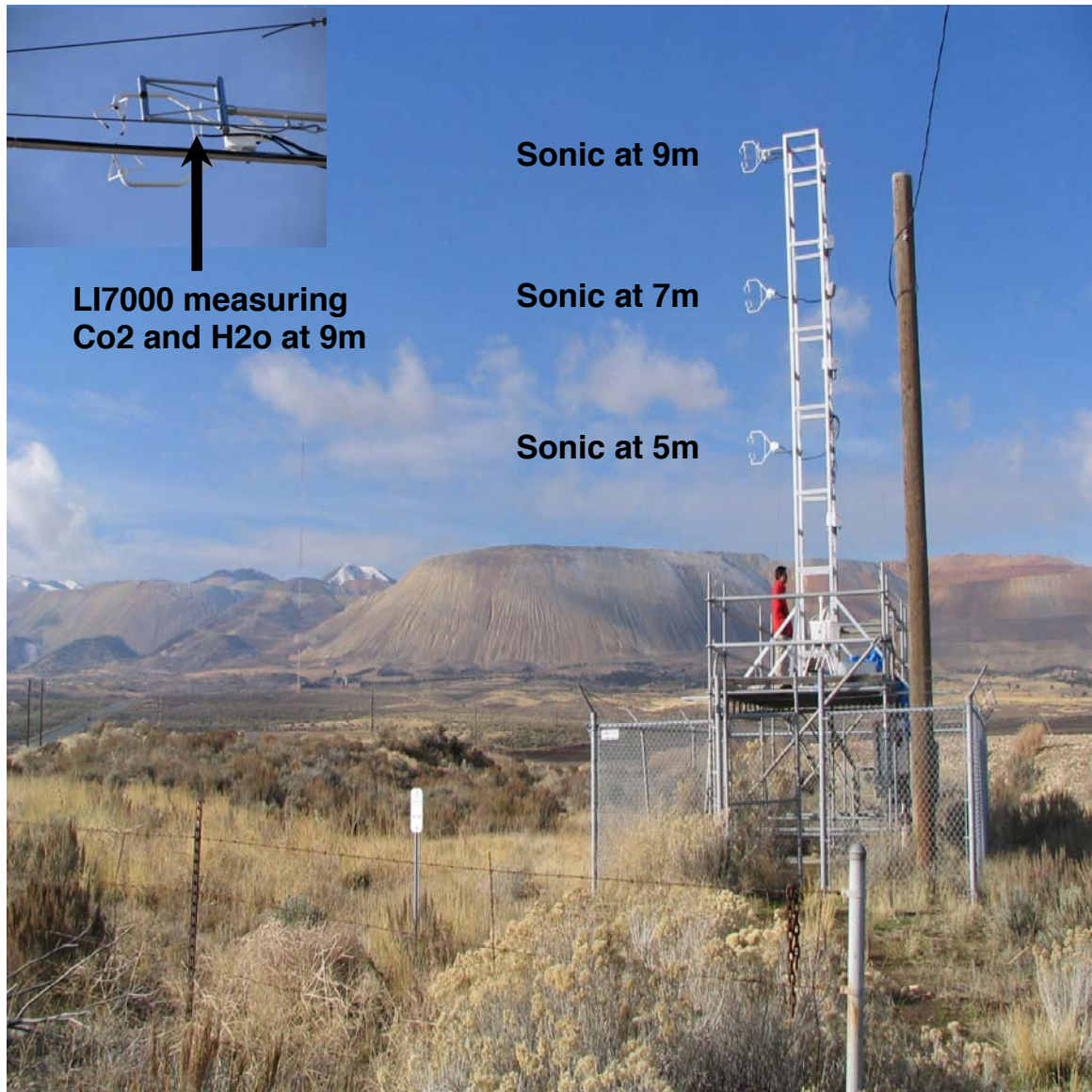


Figure 2.3 Instrumentation at the Kennecott site. The sonic anemometers point 190° .

CHAPTER 3

VALLEY METEOROLOGY

February 2004 witnessed two persistent CAP episodes, 11 through 15 February and 20 through 24 February separated by a washout event that began on 16 February and destroyed the first inversion episode by 19 February. The current chapter utilizes surface weather maps, precipitation and cloud cover along with temperature measurements from various weather monitoring stations in the Salt Lake valley to demonstrate the local weather during the two persistent inversion episodes and the washout episode.

A High pressure system that formed over the Pacific North-West approached the valley on 10 February. The high pressure system remained in place until 15 February as seen in Fig 3.1. Note that the valley was within the 32°F isotherm in Fig 3.1 which suggests that the approaching cold front from the Pacific North-West the day before may not have been responsible for filling the valley with cold air. It is possible that the CAP was formed as a result of nighttime radiative cooling. Shown in Fig 3.2 are 24 hour precipitation averages for the first inversion episode. Clearly, there is no precipitation during the first inversion episode due to presence of very little cloud cover as seen in Fig 3.3. Cloud cover during the first inversion episode as seen in Appendix confirms that the first persistent CAP episode was characterized by clear skies, good visibility also seen Fig 3.4 and very little precipitation.

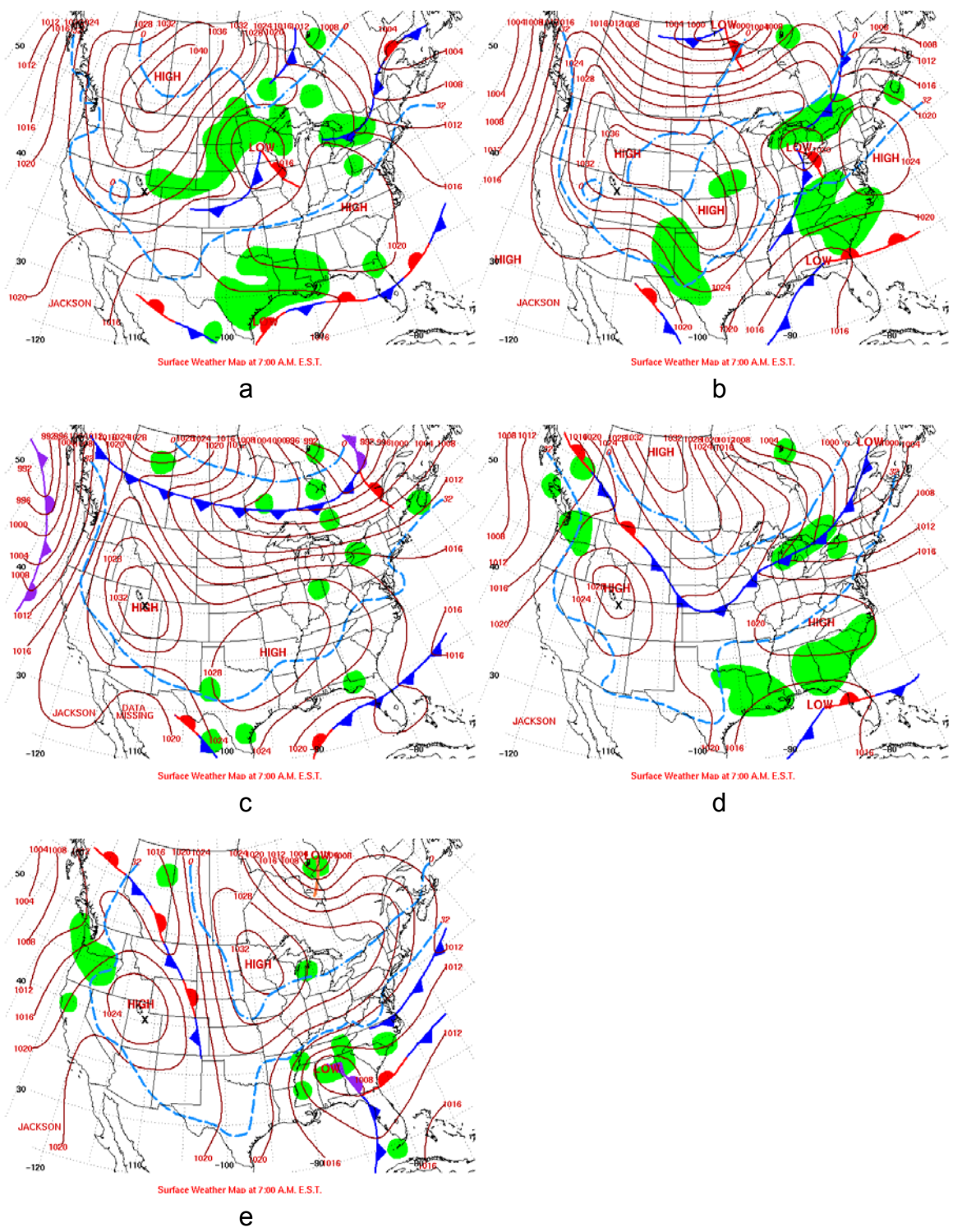


Figure 3.1 Surface weather maps at 0500 LST on (a) 11 Feb (b) 12 Feb (c) 13 Feb (d) 14 Feb and (e) 15 Feb. Shaded areas indicate precipitation. The X mark indicates the Kennecott Site. Dashed lines represent 32°F and 0°F isotherms.

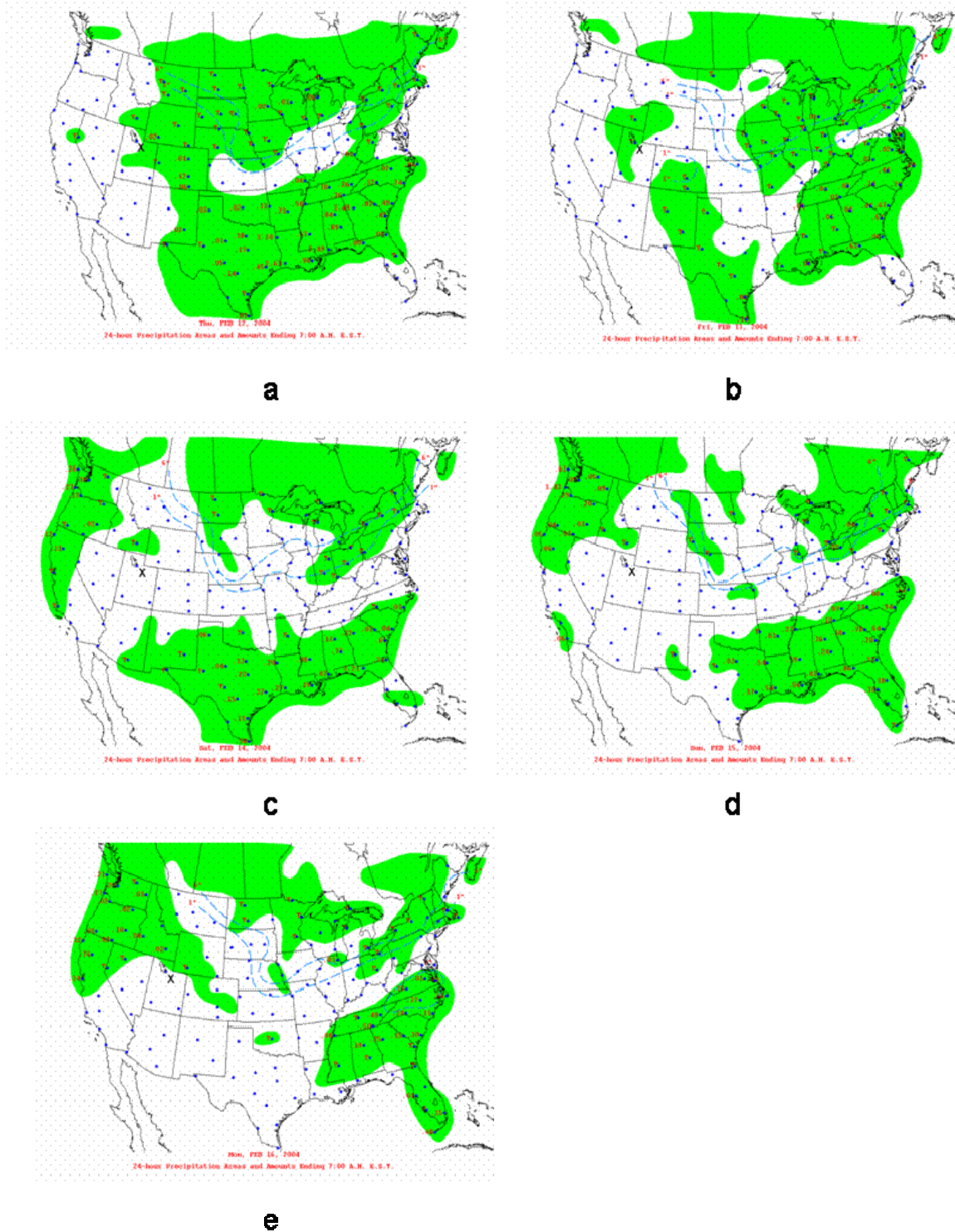


Figure 3.2 24 hour average of precipitation on (a) 11 Feb (b) 12 Feb (c) 13 Feb (d) 14 Feb and (e) 15 Feb. Shaded areas indicate precipitation with precipitation amount in inches. The X mark indicates the Kennecott Site.

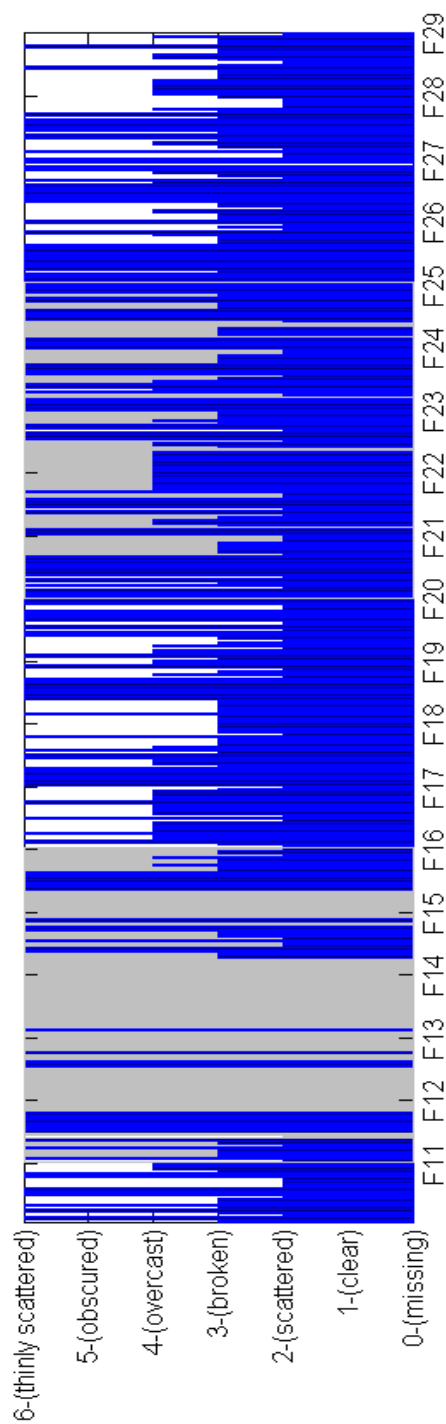
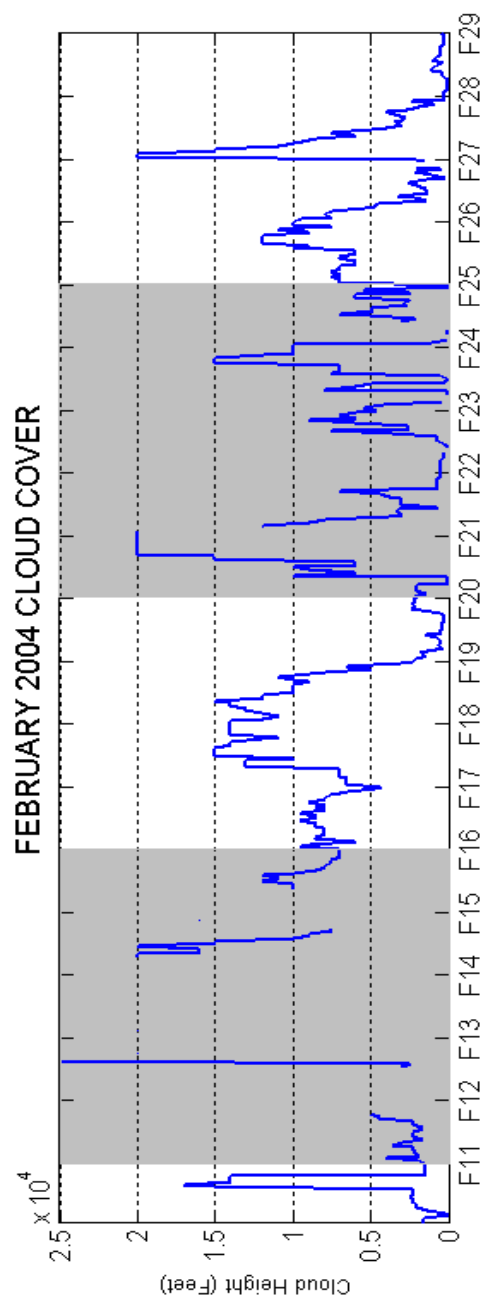


Figure 3.3 1 hour average of cloud height and cloud type from 10 through 29 February 2004 from National Weather Service. The shaded regions represent the inversion episodes.

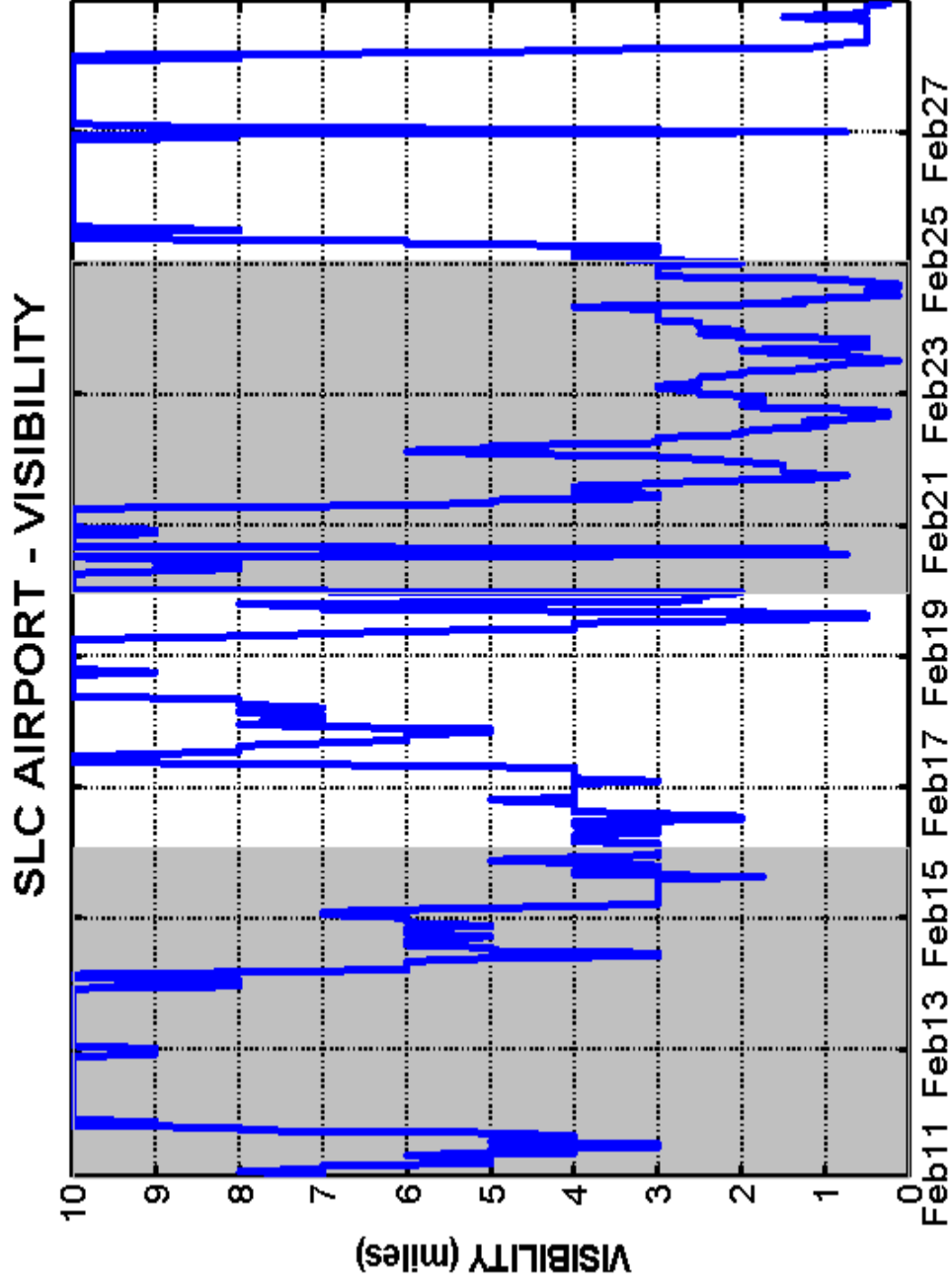


Figure 3.4 1 hour average of visibility from 11 through 29 February 2004 from National Weather Service. The shaded regions represent the inversion episodes.

Since, rawinsonde data from SLC Airport is obtained only twice everyday, temperature variations from three weather monitoring stations located at different elevations were chosen in order to analyze the vertical mixing within the valley. Time series of temperature from lowest point in the valley (SLC Airport-1288 m ASL), above the valley floor (Baccus-1576 m ASL) and at a high elevation station (Empires Peak-2750 m ASL), shown in Fig 3.5, coupled with twice a day rawinsonde data from the SLC Airport are analyzed. Fig 3.6 shows the time series of temperature from the three stations described above and rawinsonde sounding from SLC Airport at 0500 hrs LST and 1700 hrs LST from 11 February through 15 February. 0500 hrs LST sounding on 11 February (Fig 3.6 (a)) shows a stable layer near the surface which transitions to a well mixed layer with an elevated inversion above it in the 1700 hrs LST sounding. A clear sky for the most part of the day (Appendix A) suggests that the mixing was caused by convection at the surface which extended above the valley floor but the solar heating was insufficient to destroy the CAP. Temperature reading from the Airport before 0700 hrs LST of 12 February (Fig. 3.6 (b)) suggests the presence of a strong inversion at the surface followed by mixing due to surface heating as seen in the 1700 hrs LST sounding from the Airport. Note that the stable layer above the well mixed layer resembles the dry adiabatic lapse rate. The lowest of surface temperatures for the first persistent CAP episode were observed on 13 February as seen in Fig 3.6 (c). Notice that the temperature at Empires Peak was warmer over temperatures at the other two stations for the entire day, seen also in the soundings from the Airport. Furthermore, the maximum temperature at Empires Peak on 13 February was the highest compared to temperature at this station on other days suggesting that the cold temperatures caused the CAP to grow and increase in

height. The 0500 hrs LST sounding on 14 February (Fig. 3.6 (d)) shows a stable layer near the surface. Slightly warmer temperature at the surface compared to the previous day is responsible for mixing at the surface as seen in the 1700 hrs sounding. Similarly for 15 February (Fig. 3.6 (e)), the strong surface based inversion during the day transitions to a well mixed layer at the surface capped by an elevated inversion. Cloud cover information (Fig 3.3) indicates that this mixing is primarily caused by ‘bottom-up’ convection from solar heating at the surface. Please note that even though Empires Peak is not located within the valley, the temperature measurements from this site closely match the sounding data from the airport as seen in Fig 3.6. This is indicative of similar weather patterns inside and outside of the valley. Hence, the Empires Peak station was chosen for a high elevation station.

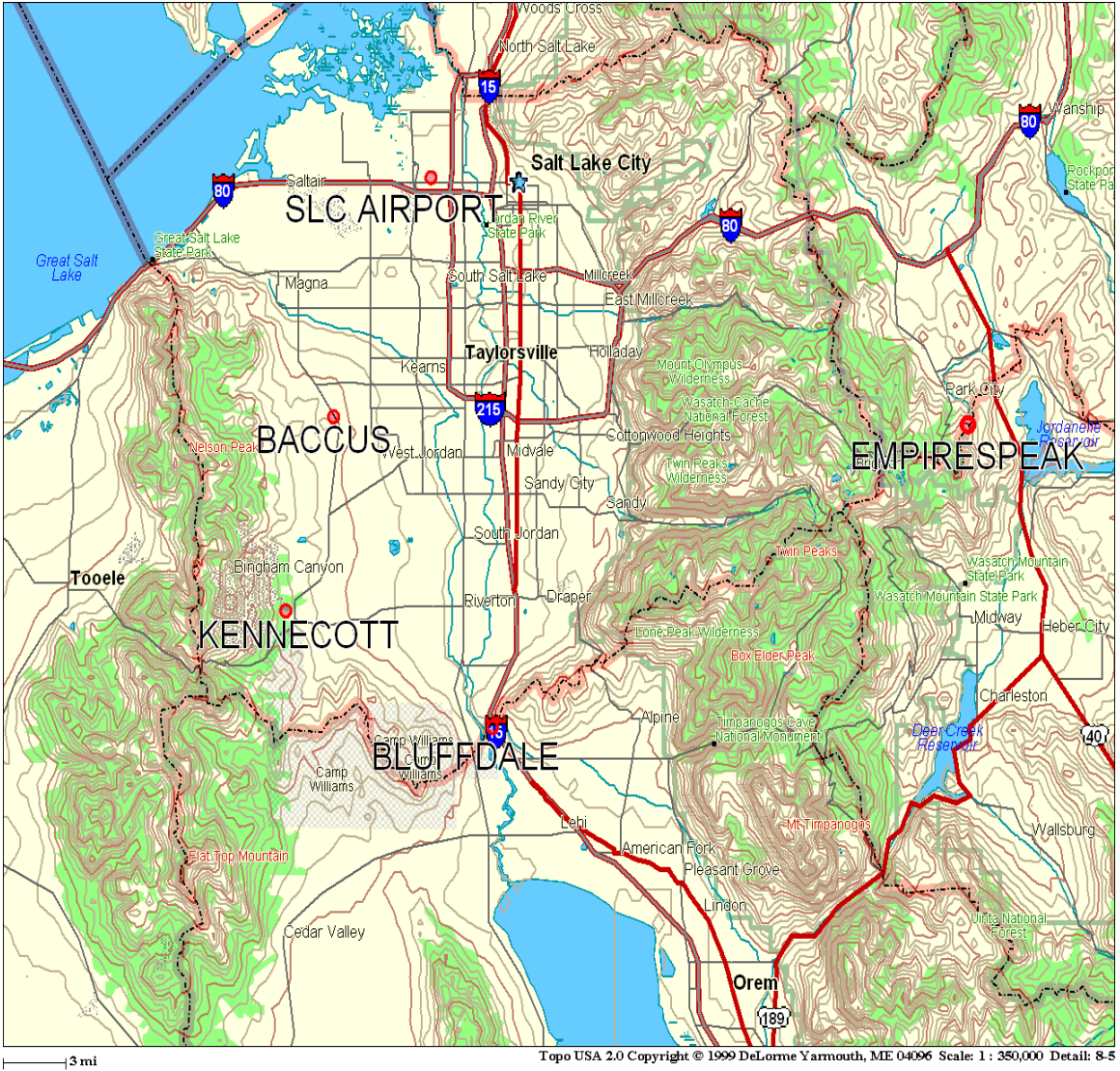


Figure 3.5 Topographic map of Salt Lake Valley showing the mesowest stations.

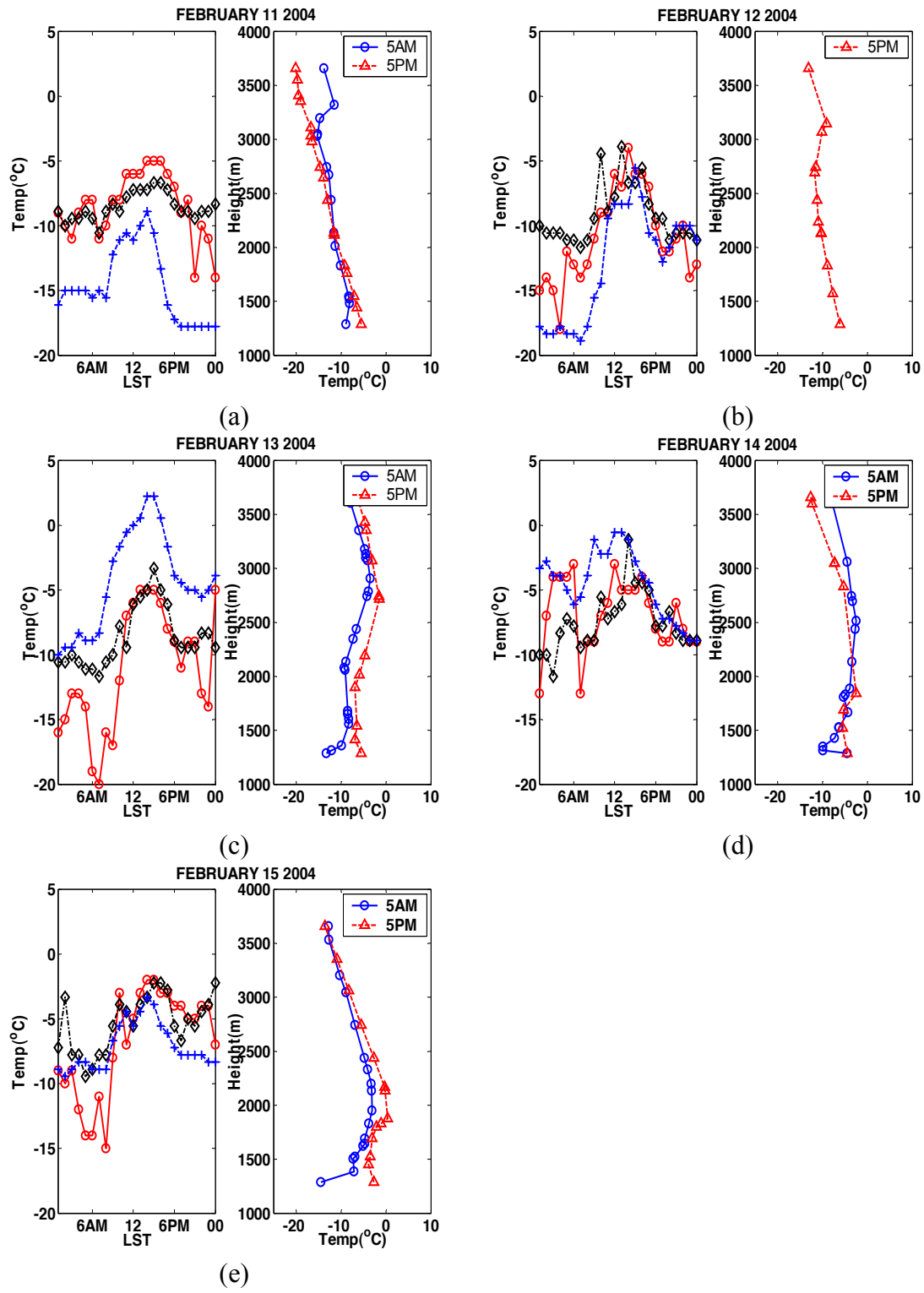


Figure 3.6. Hourly average of temperature from SLC Airport (1288m ASL, 'o'), Baccus (1576m ASL, '◇'), EmpiresPeak (2750m ASL, '+') and sounding at 0500 hrs LST and 1700 hrs LST from SLC Airport on (a)11 Feb (b)12 Feb (c)13 Feb (d)14 Feb and (e)15 Feb.

Following the first persistent CAP episode from 11 through 15 February, there was a washout mechanism caused by strong winds blowing from the South-South East direction. Fig 3.7 shows the surface weather maps from 16 through 19 February. The high pressure system that formed on 10 February continues its influence on 16 February and moves north-west by 17 February as seen in Fig 3.7 (b). Notice that the valley is not encompassed by the 32°F isotherm on 18 February (Fig 3.7 (c)). Advection of warm southerly winds is hypothesized to be the possible mechanism for the destruction of the first persistent CAP episode. Note that the washout was accompanied by precipitation on 18 through 19 February as shown in Fig 3.8 (c) and Fig 3.8 (d) respectively. 4 hour averages of temperature, relative humidity, wind speed and wind direction from Baccus/SR111 automatic weather station is shown in Fig 3.9. Notice the high wind speeds of approximately 10 ms^{-1} blowing from South-South East direction on 17 through 18 February.

Figure 3.10 shows the times series of temperature from the SLC Airport, Baccus and Empires Peak along with 0500 hrs LST and 1700 hrs LST sounding from SLC Airport from 16 through 19 February. The temperatures on 16 and 17 February exhibit a steady increase caused due to the warm winds blowing from the south. The temperatures at all stations begin decreasing on late 18 February. Also, a strong similarity of vertical profiles of temperature can be seen on 17 February and 18 February, indicative of the warm southerly flow eroding the top of the inversion. The absence of an elevated or near surface stratified layer on 19 February suggests the destruction of the persistent cold pool due to the advection of warm southerly winds.

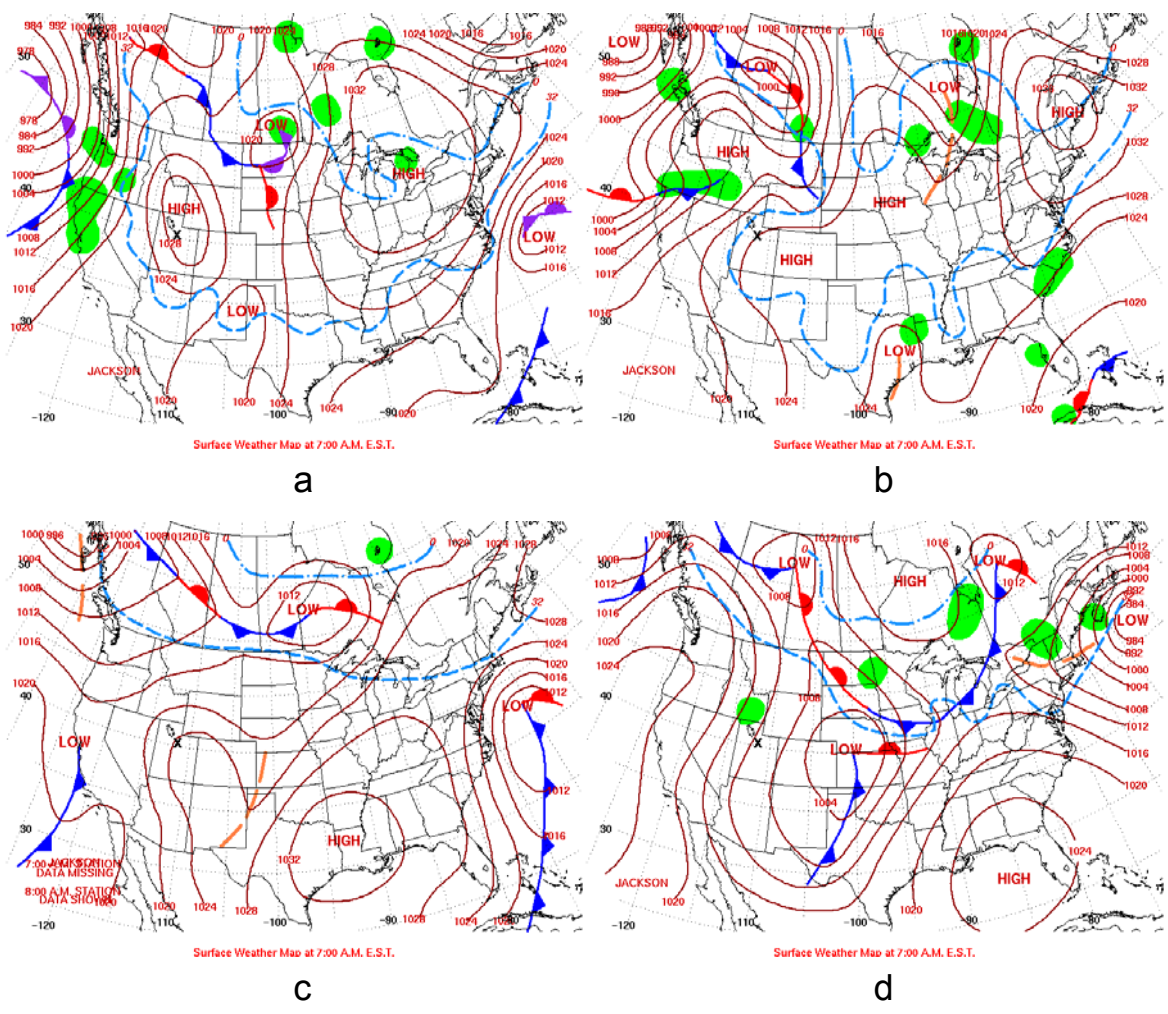


Figure 3.7 Surface weather maps at 0500 LST on (a) 16 Feb (b) 17 Feb (c) 18 Feb and (d) 19 Feb. Shaded areas indicate precipitation. The X mark indicates the Kennecott Site. Dashed lines represent 32°F and 0°F isotherms.

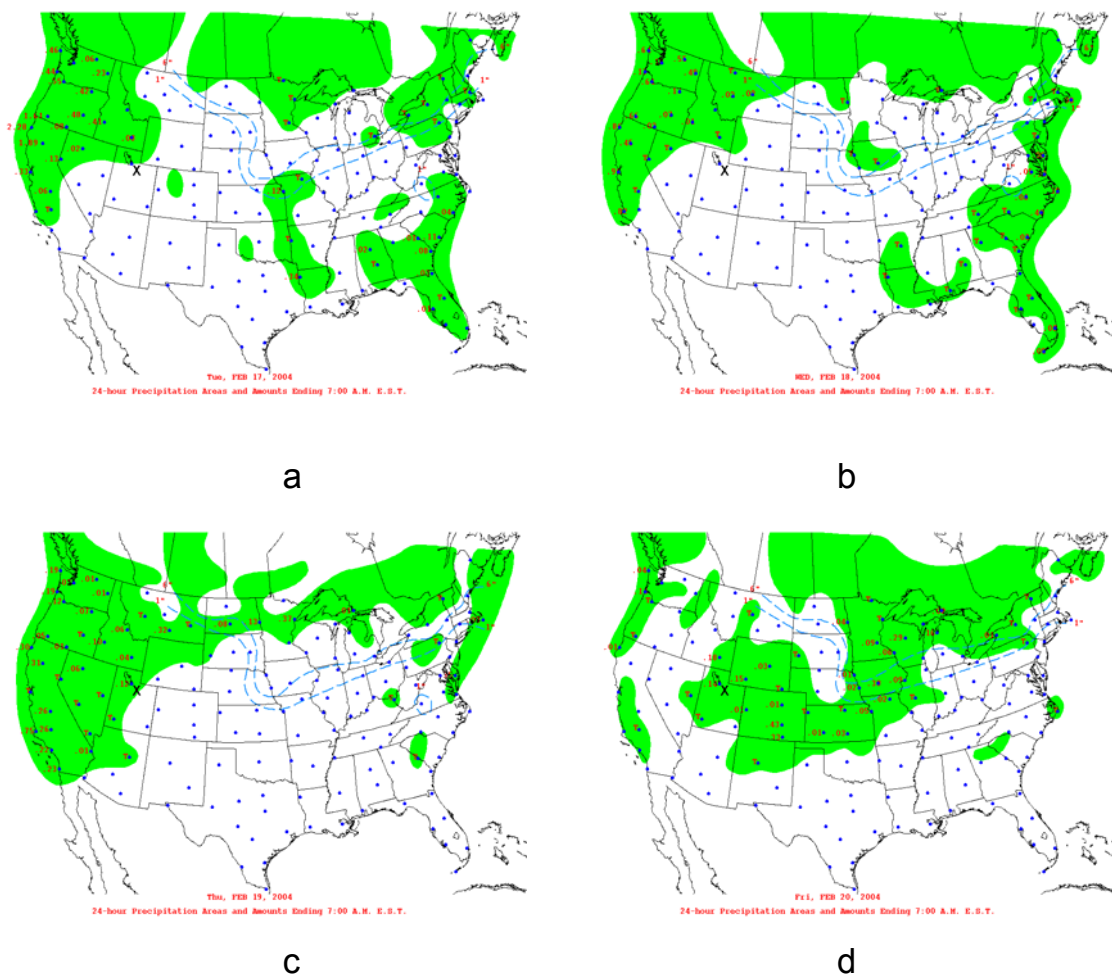


Figure 3.8 24 hour average of precipitation on (a) 16 Feb (b) 17 Feb (c) 18 Feb (d) and 19 Feb. Shaded areas indicate precipitation with precipitation amount in inches. The X mark indicates the Kennecott Site.

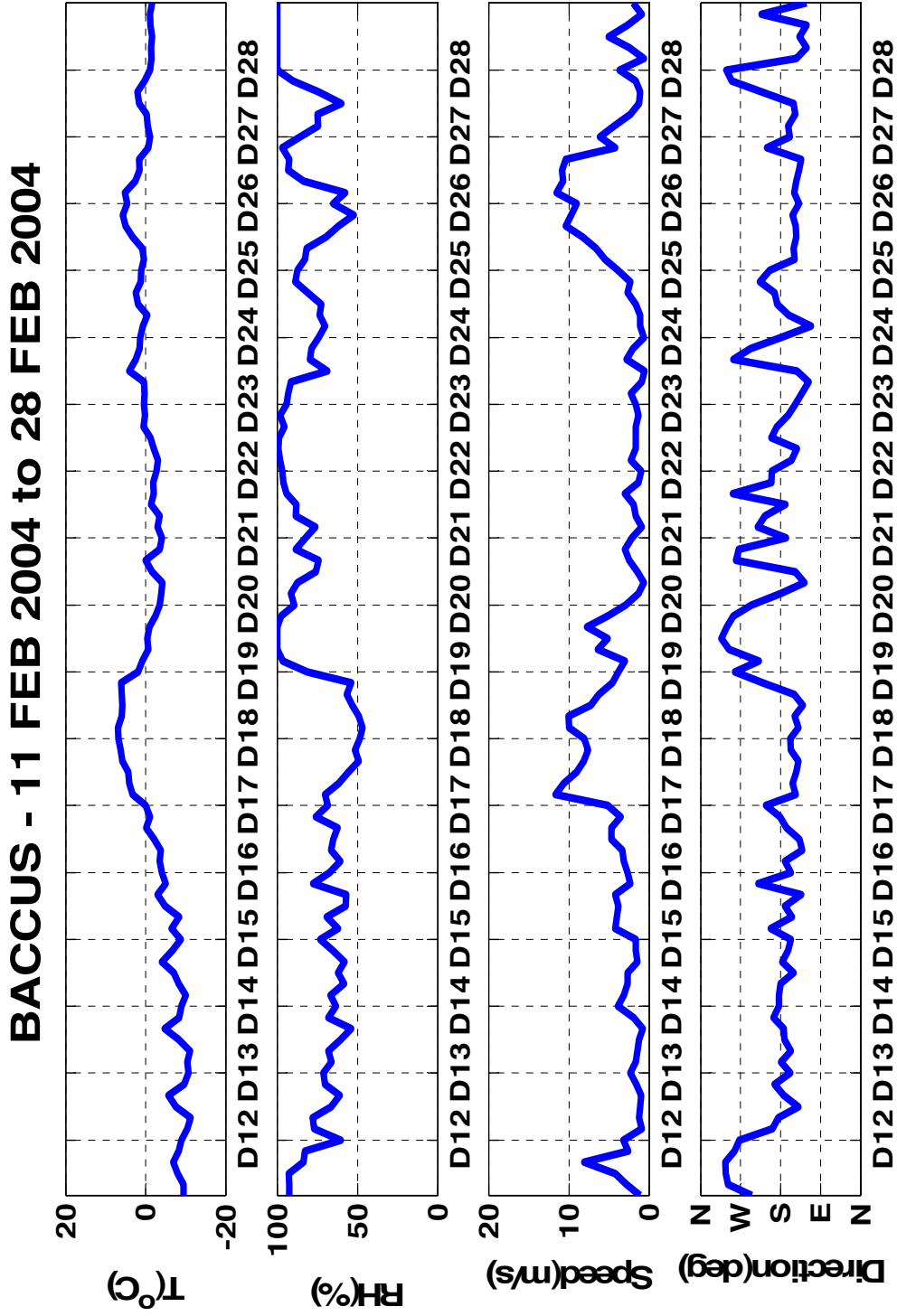


Figure 3.9 4 hour average of temperature, relative humidity, wind speed and wind direction from 11 through 28 February 2004 collected from Baccus/SR111(BAC) station..

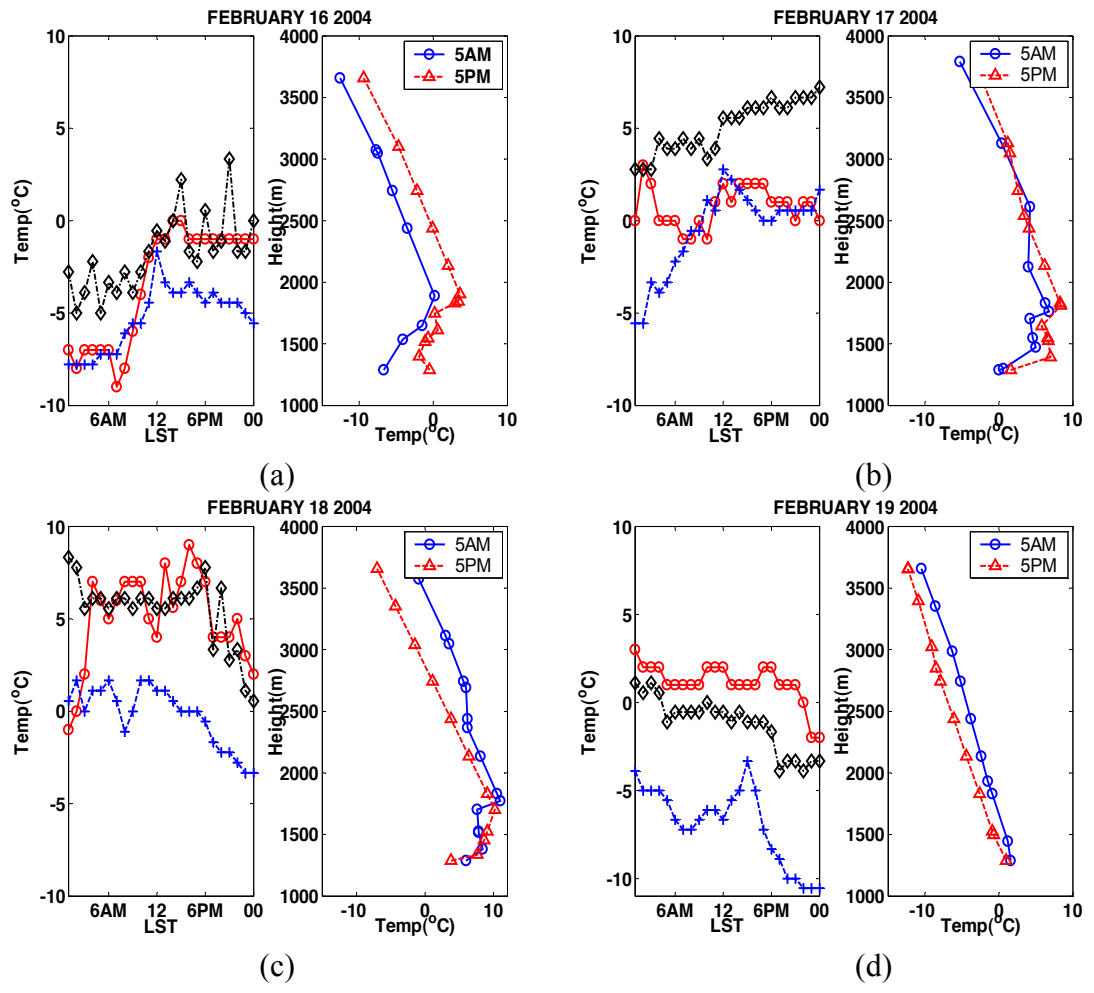


Figure 3.10. Hourly average of temperature from SLC Airport (1288m ASL, 'o'), Baccus (1576m ASL, '◇'), EmpiresPeak (2750m ASL, '+') and sounding at 0500 hrs LST and 1700 hrs LST from SLC Airport on (a)16 Feb, (b)17 Feb, (c)18 Feb and (d)19 Feb.

Following the washout event that began on 16 February and destroyed the first persistent CAP episode by 19 February, a second episode began on 20 February. Seen in Fig 3.11 are the surface weather maps for the second persistent CAP from 20 through 24 February. Notice that the valley is within the 32°F isotherm on all days. The valley was under the influence of low pressure systems on all days but 20 February as seen in Fig 3.11 (a). The valley meteorology for the second episode was mostly characterized by low cloud cover as seen in Fig 3.3 and precipitation (fig 3.12). This is confirmed by the cloud cover pictures at 0700 hrs LST, 1000 hrs LST, 1300 hrs LST and 1600 hrs LST from 20 through 24 February in Appendix A. The pictures also portray very poor visibility especially on 21 through 22 February also seen in Fig 3.4.

Shown in Fig 3.13 is the time series of temperature from three stations namely SLC Airport at 1288m ASL, Baccus at 1576m ASL and Empires Peak located at 2750m ASL and twice a day sounding data from SLC Airport from 20 through 24 February. The sounding data for 20 February in Fig 3.13 (a) suggests that there was surface based inversion in the morning that transformed into a well mixed layer capped by an elevated inversion. With clear skies and clear visibility on this day, the vertical mixing may have been caused from solar heating of the surface ('bottom-up' convection). The vertical profiles of temperature on 21 February (Fig 3.13 (b)) follow the transition from a strong surface based inversion to a well mixed layer capped by elevated inversion similar to the previous day. Since the local weather on 21 February was characterized by poor visibility, and low cloud cover, convection from 'top-down' may explain the mixing near the surface. Notice the 0500 hrs LST sounding and 1700 hrs LST sounding on 22 February appear to be very similar with mixing near the surface and elevated inversion on

top of this mixed layer. The local weather on 22 February was similar to the previous day with very poor visibility and overcast conditions which may suggest that the ‘top-down’ continued from 21 through 22 February (Fig 3.13 (c)). The surface based inversion on 23 through 24 February seen in Fig 3.13 (d) and Fig 3.13 (e) can be explained by the cloud cover information. Both days were characterized with mostly scattered and broken clouds which may have prevented the occurrence of ‘top-down’ convection. The surface temperatures were much warmer the following day and the absence of surface based inversion suggested the washout of the second persistent CAP episode.

To summarize, there were two persistent CAP episodes in February 2004, 11 through 15 February and 20 through 24 February that were separated by a washout mechanism between 16 and 19 February. Night time radiative cooling may be responsible for the formation of the two episodes while the destruction was caused by the advection of warm winds blowing from South-South East direction. It is important to note that both inversion episodes displayed similar characteristics with a surface based inversion transitioning to a well mixed layer near the surface capped by an elevated inversion. However, the local weather for both episodes was distinctly different. The first episode was characterized by clear skies, good visibility and no precipitation while the second episode was characterized by overcast conditions and very poor visibility. This suggests that the vertical mixing for the first episode was caused by the solar heating at the surface or ‘bottom-up’ convection and the mixing during the second episode was caused by the convection from cloud base to the surface or ‘top-down’ convection.

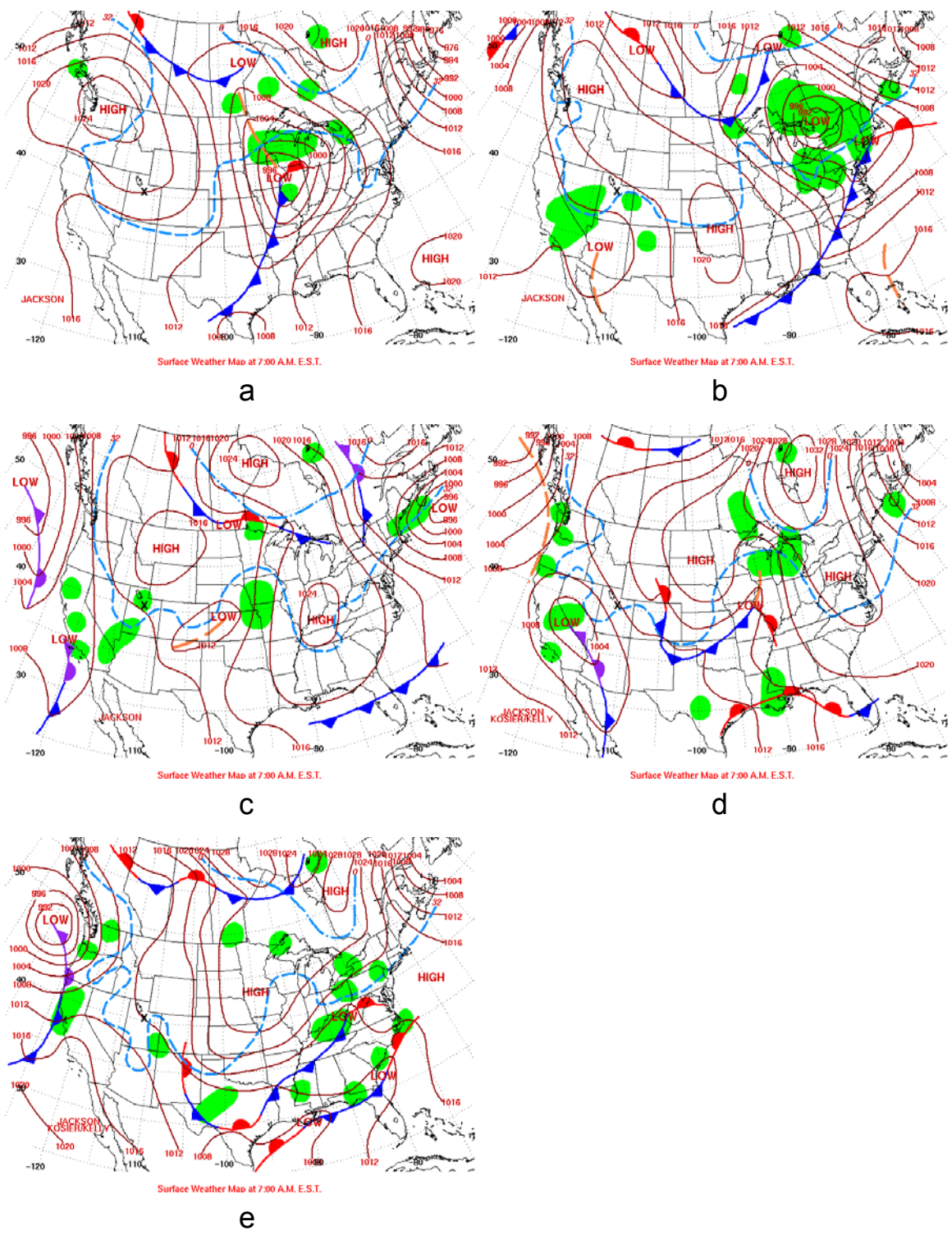


Figure 3.11 Surface weather maps at 0500 LST on (a) 20 Feb (b) 21 Feb (c) 22 Feb (d) 23 Feb and (e) 24 Feb. Shaded areas indicate precipitation. The X mark indicates the Kennecott Site. Dashed lines represent 32°F and 0°F isotherms.

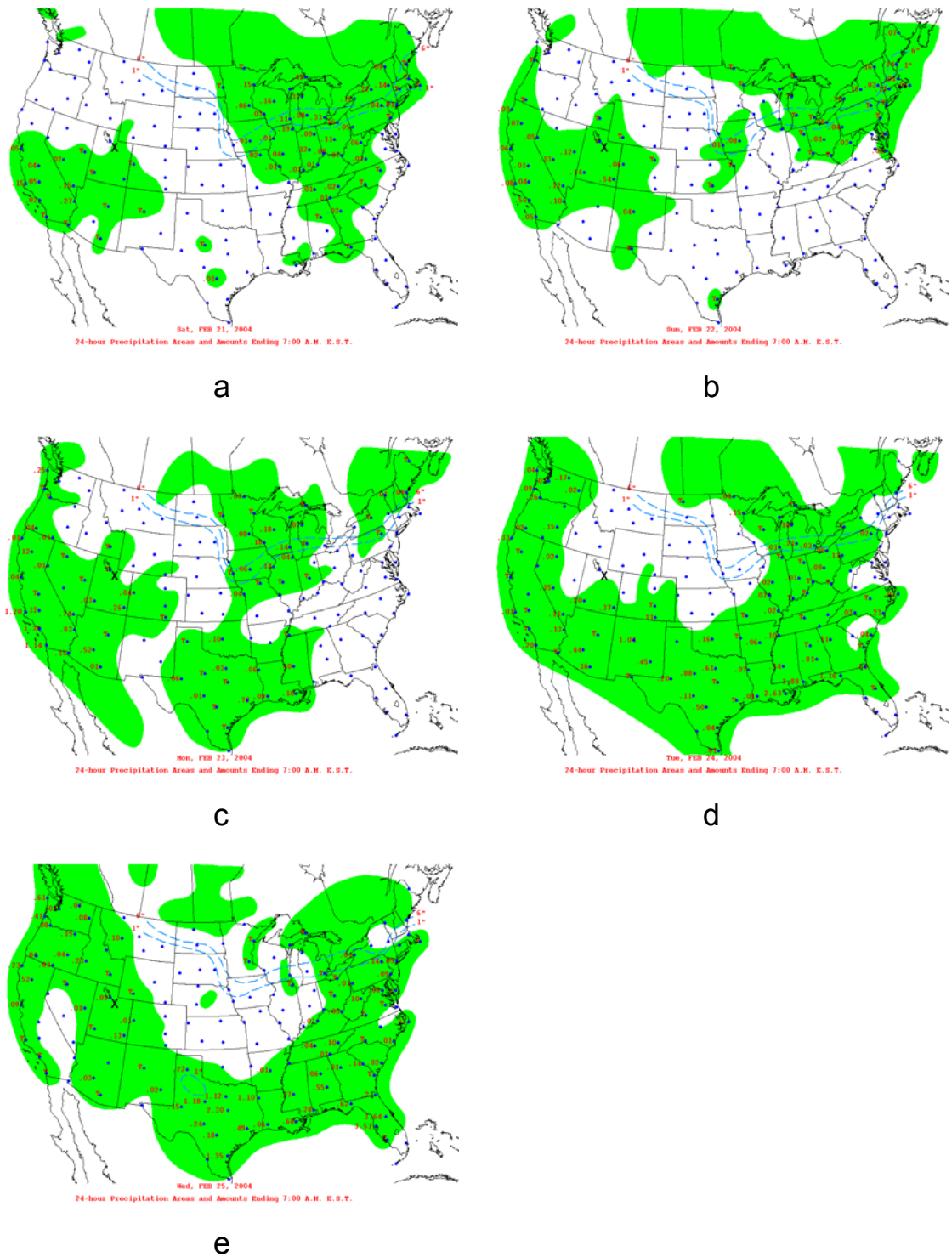


Figure 3.12 24 hour average of precipitation on (a) 20 Feb (b) 21 Feb (c) 22 Feb (d) 23 Feb and (e) 24 Feb. Shaded areas indicate precipitation with precipitation amount in inches. The X mark indicates the Kennecott Site.

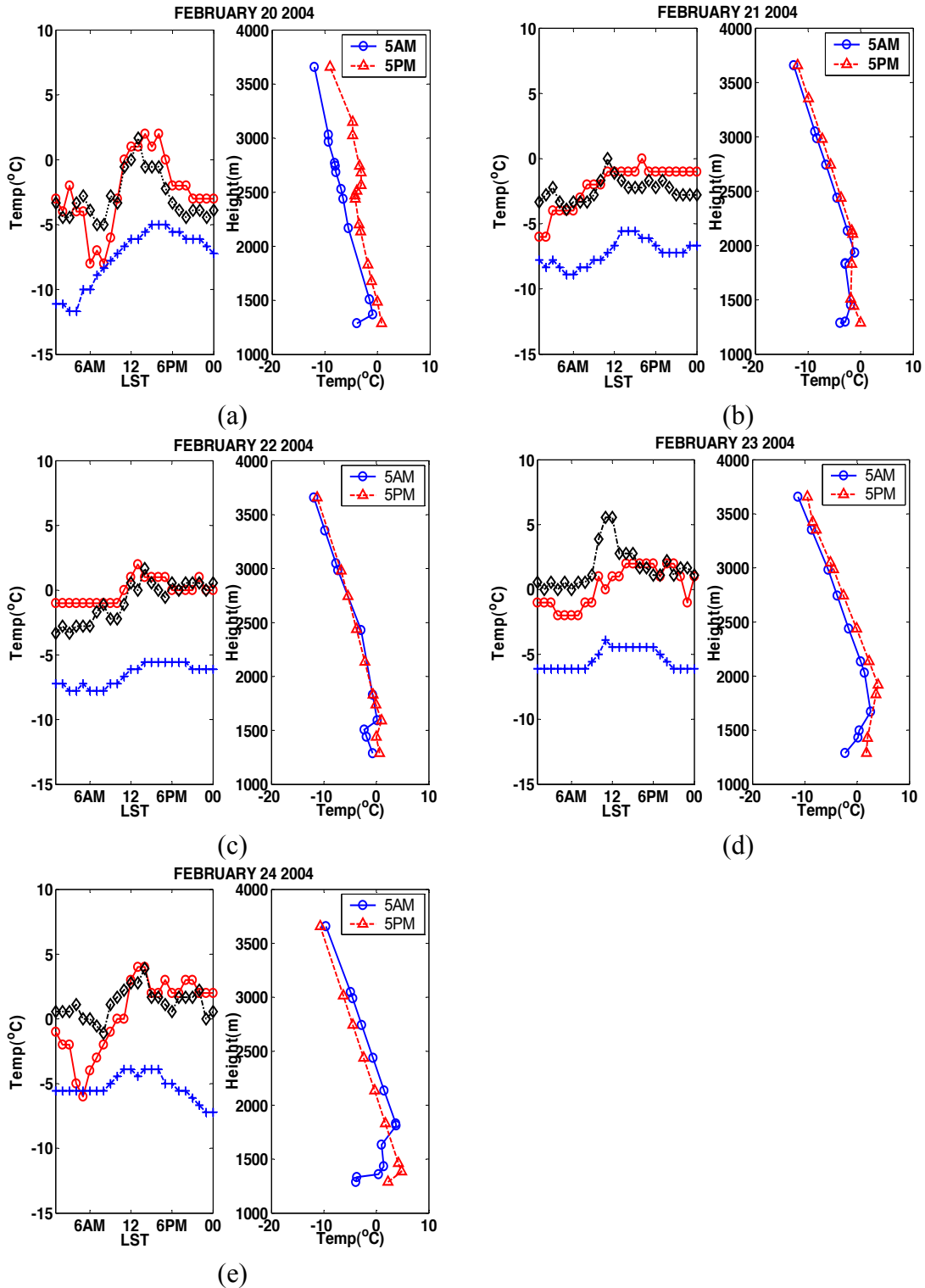


Figure 3.13. Hourly average of temperature from SLC Airport (1288m ASL, 'o'), Baccus (1576m ASL, '◇'), EmpiresPeak (2750m ASL, '+') and sounding at 0500 hrs LST and 1700 hrs LST from SLC Airport on (a)20Feb (b)21 Feb (c)22 Feb (d)23 Feb and (e)24 Feb.

The temperature measurements from Airport, Baccus and Empires peak along with the sounding data from the airport clearly suggest the presence of two types of cold pools. A surface based inversion called ‘Type 1’ and a well mixed layer near the surface capped by an elevated inversion called ‘Type 2’. These two types of cold air pool scenerios are shown in Fig. 3.14. It was observed that both the episodes displayed a transition of ‘Type 1’ scenario to a ‘Type 2’ scenario. Fig 3.15 depicts the distribution of the ‘Type 1’ and ‘Type 2’ cold air pool scenario from 11 through 28 February 2004.

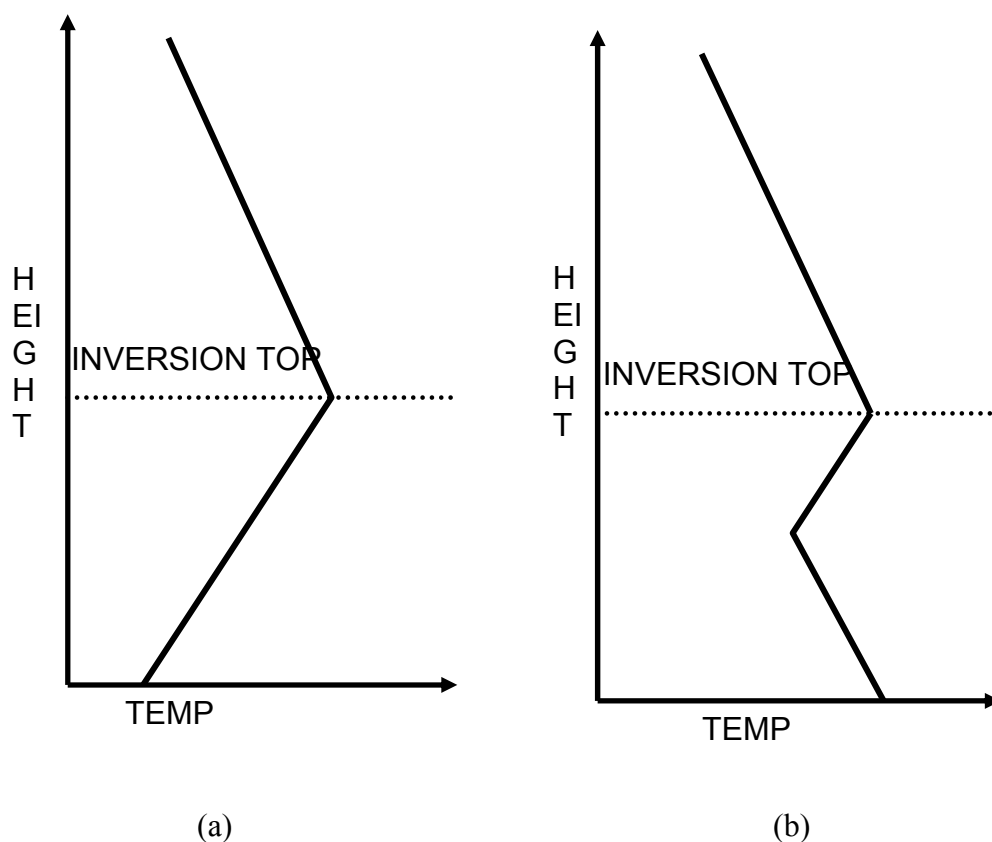


Figure 3.14. Two types of cold air pool mixing scenerios. (a) Surface based inversion or ‘Type 1’. (b) Well mixed layer near the surface capped by an elevated inversion or ‘Type 2’.

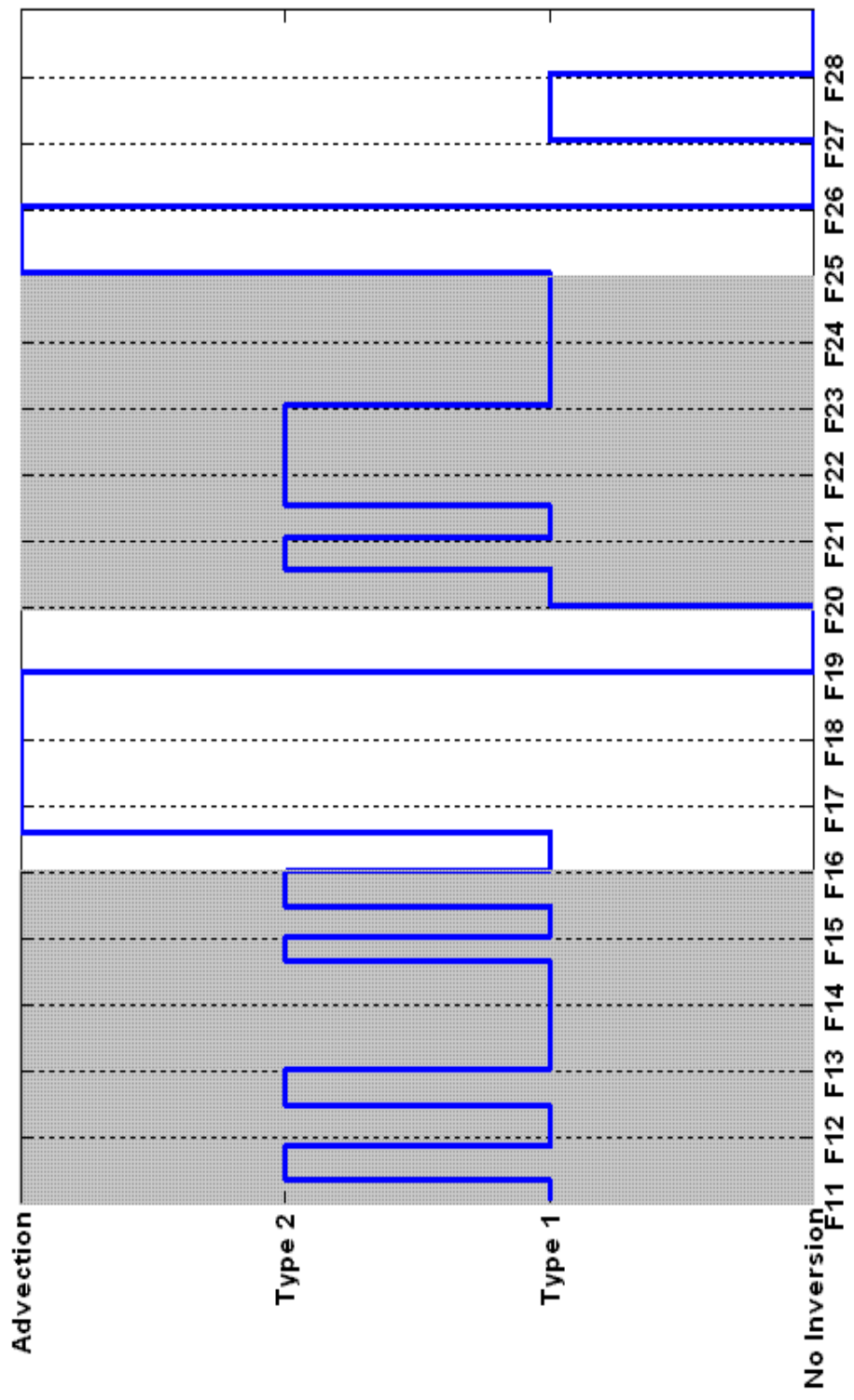


Figure 3.15 Type1 and Type 2 scenario fom 11 February 2004 through 28 February 2004. Shaded areas indicate the two persistent inversion episodes.

CHAPTER 4

LOCAL TURBULENCE

4.1 Monthly Average

CSAT 3 Sonic Anemometers measured wind velocities in the axial, transverse and vertical direction along with temperature at 9.16 m AGL at a frequency of 10 Hz. The measurements are linearly detrended over a 5 minute window and averaged over a 30 minute time period. The Planar Fit Method by Wilczak et al. (2001) was used to remove the effects of surface inclination. Figure 4.1 shows the daily mean velocity and temperature from 11 through 29 February 2004. Mean velocities can be seen to be small during the two persistent cold pool episodes from 11 through 15 February and 20 through 24 February due to the mountains that act as barriers and inhibit the movement of cold air in the valley. Advection of warm air from the south produced relatively higher wind velocities near the surface on 17 and 25 February. The temperatures during the second inversion episode were higher than the first persistent inversion episode. Warm air advection was the reason for warmer temperatures during that period.

Radiation from the sun heats the surface during daytime, generating warm thermals that raise the temperature of air near the surface. These thermals carry heat from the surface to the surrounding air due to the temperature gradient between the air and the surface. This flux of heat from the surface is called the sensible heat flux defined as,

$$H_s = \rho c_p \overline{W'T'}, (\text{W/m}^2)$$

where, ρ = density of air (kg/m^3)

c_p = specific heat of air (J/kg K)

W' = Turbulent fluctuation of velocity in the vertical direction. (m/s)

T' = Turbulent fluctuation of temperature. (K)

The flux of sensible heat is positive when the surface is at a higher temperature than the overlying air and it is negative when heat is transferred from air toward the surface. Figure 4.1 shows the daily averages of sensible heat flux from 11 through 29 February 2004. Low daily averages of sensible heat flux during the persistent inversion episodes indicate the daily radiation from the sun was insufficient to raise the temperature of the surface and destroy the persistent inversion. High negative sensible heat flux on 17, 18 and 25 February are due to the advection of warm air over the surface.

Turbulent shear stress is the product of turbulent fluctuations of velocities in the along wind and vertical direction. Mathematically, turbulent shear stress is defined as

$$\text{Shear stress} = \overline{U'W'}, (\text{m}^2/\text{s}^2)$$

where, U' = Turbulent fluctuation of velocity in the along wind direction, (m/s)

W' = Turbulent fluctuation of velocity in the vertical direction. (m/s)

The average maximum value of shear stress during a typical day would be $-0.1\text{m}^2/\text{s}^2$. The shear stress is always negative because the surface acts as a sink of momentum. Figure Seen in Fig 4.1 is the daily average of shear stress from 11 through 29 February. Low shear stress during the persistent inversion episodes indicates low turbulence. High shear near the surface on 17, 18, 25 and 26 February was caused from advection of warm air from the south.

Turbulent Kinetic Energy (TKE) is a direct measure of the intensity of turbulence. It is directly related to momentum, heat and moisture transport through the boundary layer (Stull, 1988). It is defined as,

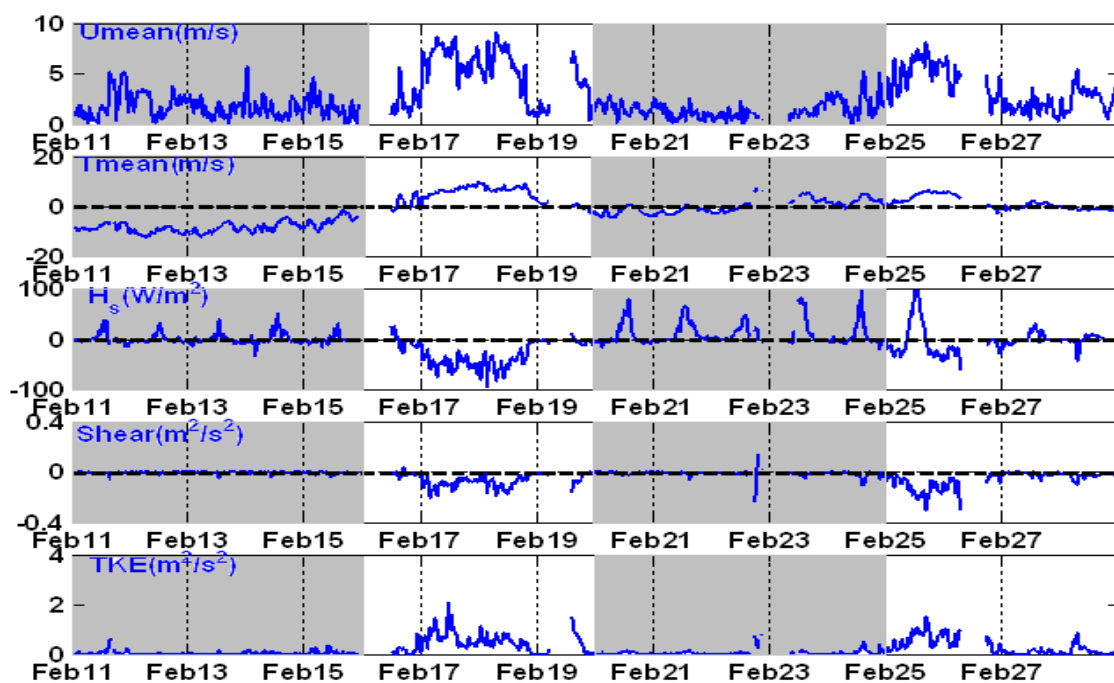
$$\text{TKE} = 0.5 * \left[\overline{U'^2} + \overline{V'^2} + \overline{W'^2} \right] (\text{m}^2/\text{s}^2),$$

where, U' = Turbulent fluctuation of velocity in the along wind direction, (m/s)

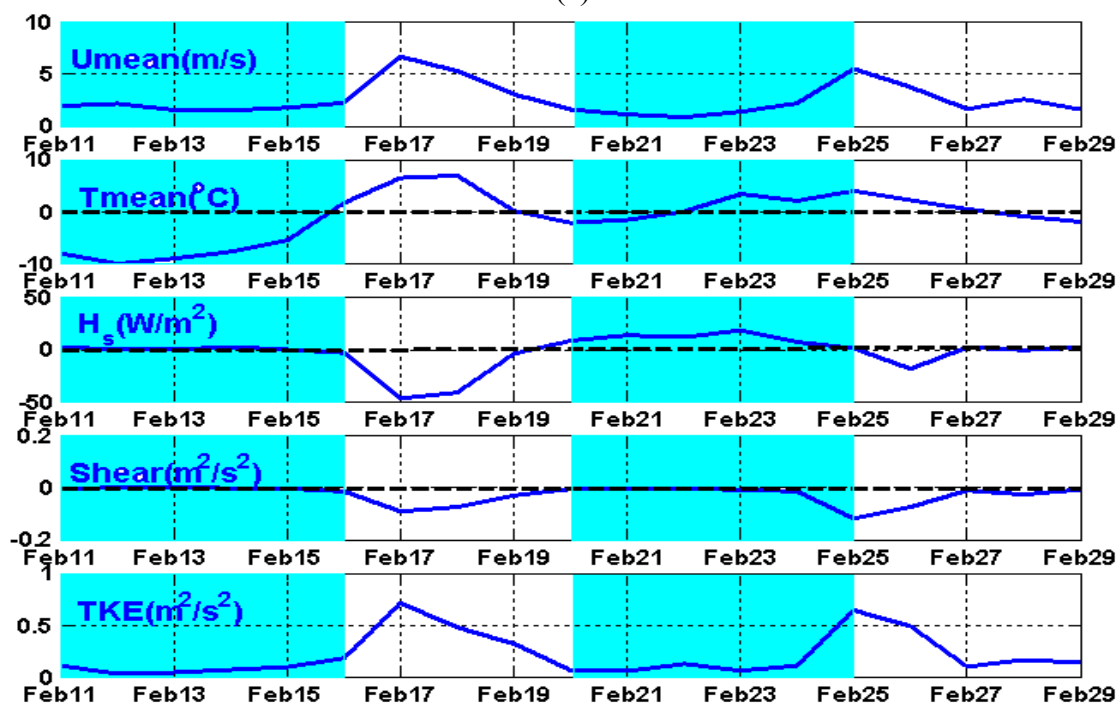
V' = Turbulent fluctuation of velocity in the transverse direction, (m/s)

W' = Turbulent fluctuation of velocity in the vertical direction. (m/s)

The average maximum value of TKE during a typical daytime period is approximately $1\text{ m}^2/\text{s}^2$. Figure 4.1 shows the daily averages of TKE from 11 through 29 February 2004. Very small daily averages during both persistent inversion episodes indicate low turbulent activity in the boundary layer. Advection of warm air from the south on 17, 18, 24 and 25 February 2004 generated huge shear near the surface.



(a)



(b)

Figure 4.1 (a) 30 minute and (b) Daily averages of along wind velocity, temperature, sensible heat flux, turbulent shear stress and turbulent kinetic energy from 11 through 29 February 2004, measured at 9.16 m AGL at Kennecott site. Shaded regions represent the persistent inversion episodes.

4.2 Warm Air Advection

The valley weather during the first persistent CAP episode from 11 through 15 February was characterized by very low fluxes of heat and momentum as discussed in the previous section. The warm air advection from south caused a rapid increase in wind speeds, temperature and fluxes of heat and momentum. Figure 4.2 shows the hourly averages of temperature, wind speed and wind direction from the Kenecott site measured at 9.16m AGL from 16 through 19 February. A rapid increase in temperature and wind speeds can be seen at around 1500 MST and 2000 MST of 16 February. The decrease in wind speed and temperature around 1800 MST on 16 February may be indicative of sloshing of warm air from the south at a time when cold air was present in the valley. A steady increase in temperature advected by south-east winds continues throughout 17 February. The sudden decrease in temperature and wind speed after around 1800 MST on 18 February is an indication of the end of the warm air advection. Temperature and wind speed at Bluffdale automatic weather station is slightly higher than temperature at the Kenecott site from 17 through 18 February (Fig 4.3) due to the fact that Kenecott site is located at a higher elevation to Bluffdale. The difference in elevation also explains the higher temperature recorded at the Kenecott site by the intruding warm air before Bluffdale on 16 February. Although Kenecott is located on a slope and Bluffdale located at the mouth of the valley both sites are under the influence of warm southerly flow from 17 through 18 February.

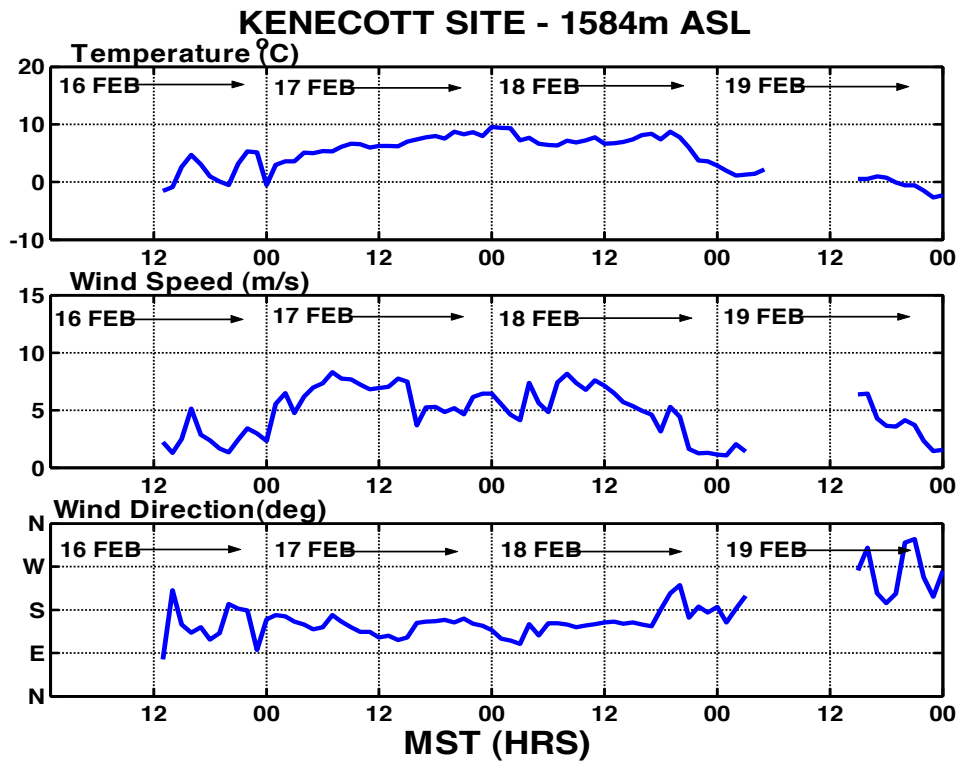


Figure 4.2 Hourly average of temperature, wind speed and direction measured at 9.16 m AGL at the Kennecott site from 16 through 19 February 2004.

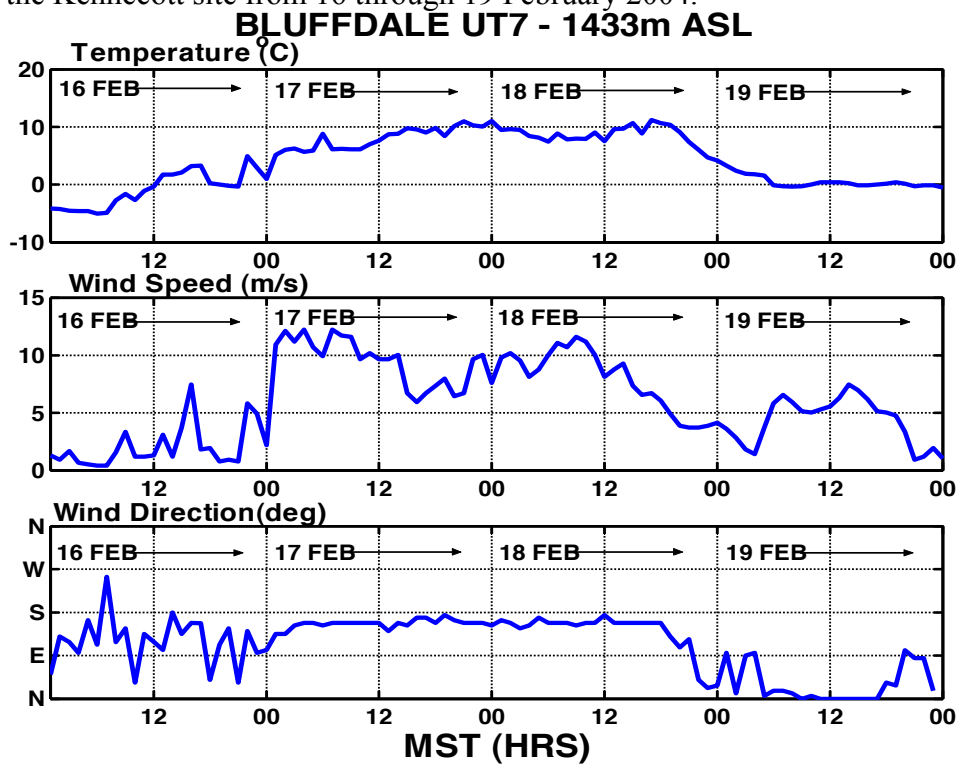


Figure 4.3 Hourly average of temperature, wind speed and direction measured at 9.16 m AGL at Bluffdale from 16 through 19 February 2004.

Figure 4.4 shows the 30 minute averages of sensible heat flux from 17 through 18 February at the Kennecott site. High negative sensible heat fluxes are suggestive of temperature differences between the surface and the air above the surface, with heat being directed towards the surface when air above the surface is warmer than the surface. The advection of warm air from the south-east generated high turbulence near the surface as seen in Figure 4.5 and 4.6. The typical maximum magnitude of turbulent kinetic energy during convective conditions is $1 \text{ m}^2/\text{s}^2$ (Stull, 1988). High turbulent kinetic energy and wind shear suggests that the turbulence generated by warm air might have scoured the top of the cold pool initiating the destruction of the persistent CAP in the valley.

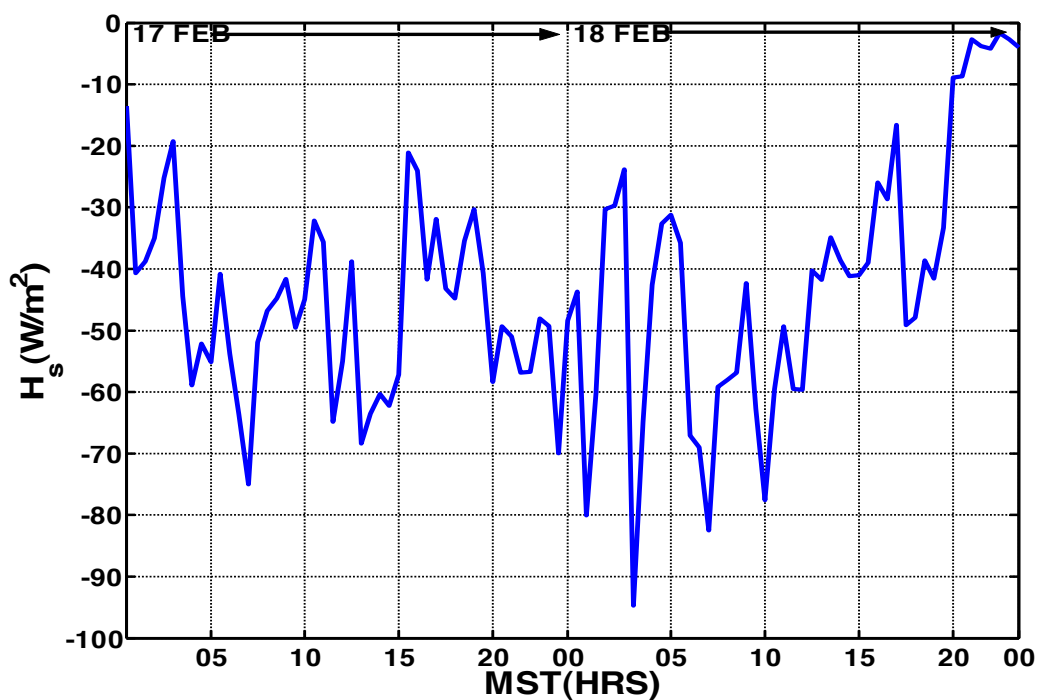


Figure 4.4 30 minute average of sensible heat flux measured at 9.16 m AGL at the Kennecott site from 17 through 18 February 2004.

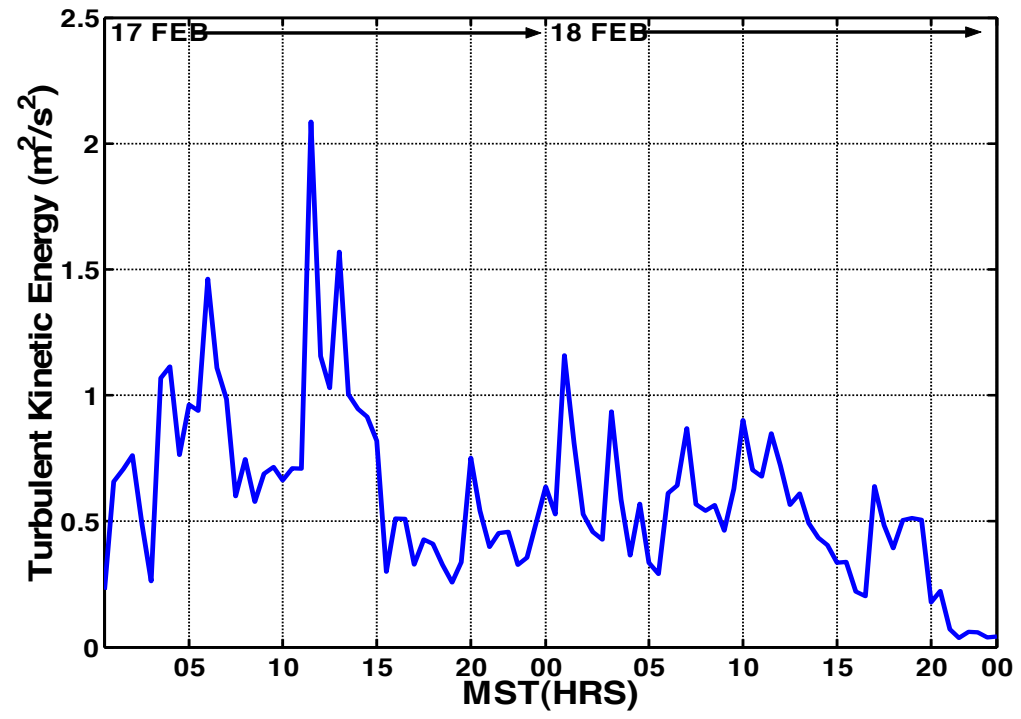


Figure 4.5 30 minute average of Turbulent Kinetic Energy measured at 9.16 m AGL at the Kennecott site from 17 through 18 February 2004.

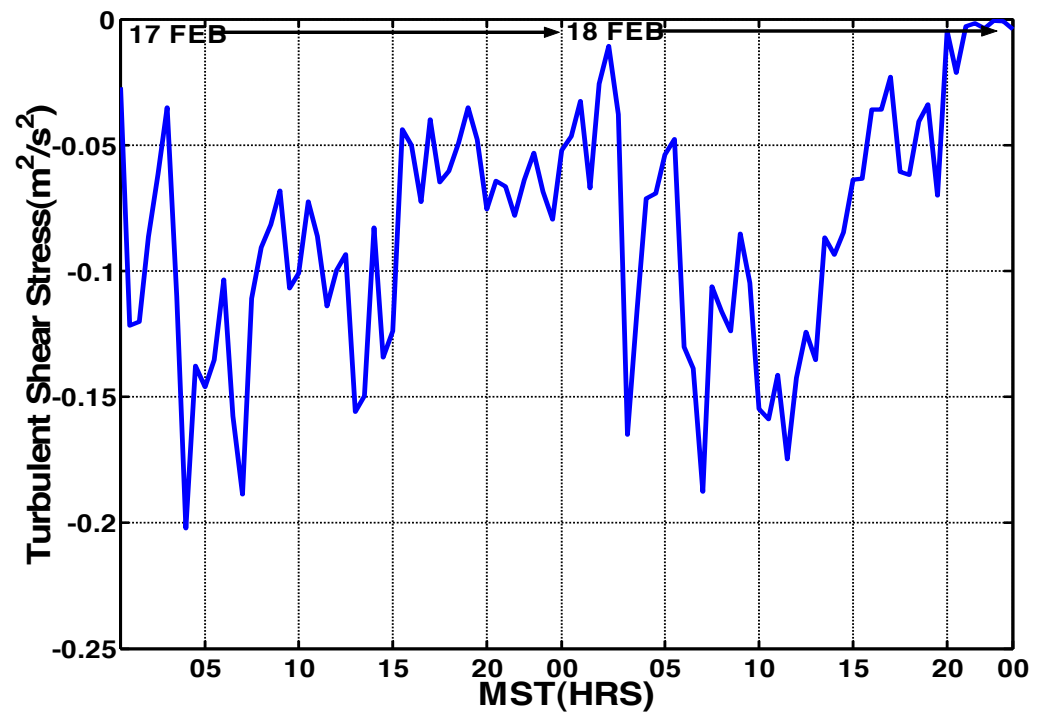


Figure 4.6 30 minute average of Turbulent Shear Stress measured at 9.16 m AGL at the Kennecott site from 17 through 18 February 2004.

4.3 Cold pool/Non Cold pool Comparison

Micrometeorological variables for the first persistent inversion episode of 11 through 15 February 2004 are compared to the micrometeorological variables from 11 through 15 March 2004. This time period in March was not under the influence of an inversion. The turbulent fluctuations are evaluated by linearly detrending the 10 Hz data from the CSAT3 sonic anemometers and LI7000 over 5 minute time periods. The turbulent variables are then block averaged for every 30 minutes. An ensemble average over the 5 day period from February and March are then compared. The variation of mean temperature range over the 5 day period in February and March 2004 is shown in Figure 4.7. The 5 day ensemble average for February clearly displays the low temperatures recorded during the first inversion episode and the temperatures increased by approximately 15°C exactly one month later. In order to investigate the variability of mean temperature with and without the inversion 5 day ensemble average of normalized temperature, defined as $T_s - T_{s,mean}$ was plotted for the first persistent inversion episode in February and compared to 5 day ensemble average during March when there was no inversion as seen in Figure 4.8. Clearly, the persistent inversion episode displays lower mean temperature variability when compared to a time period when there was no inversion.

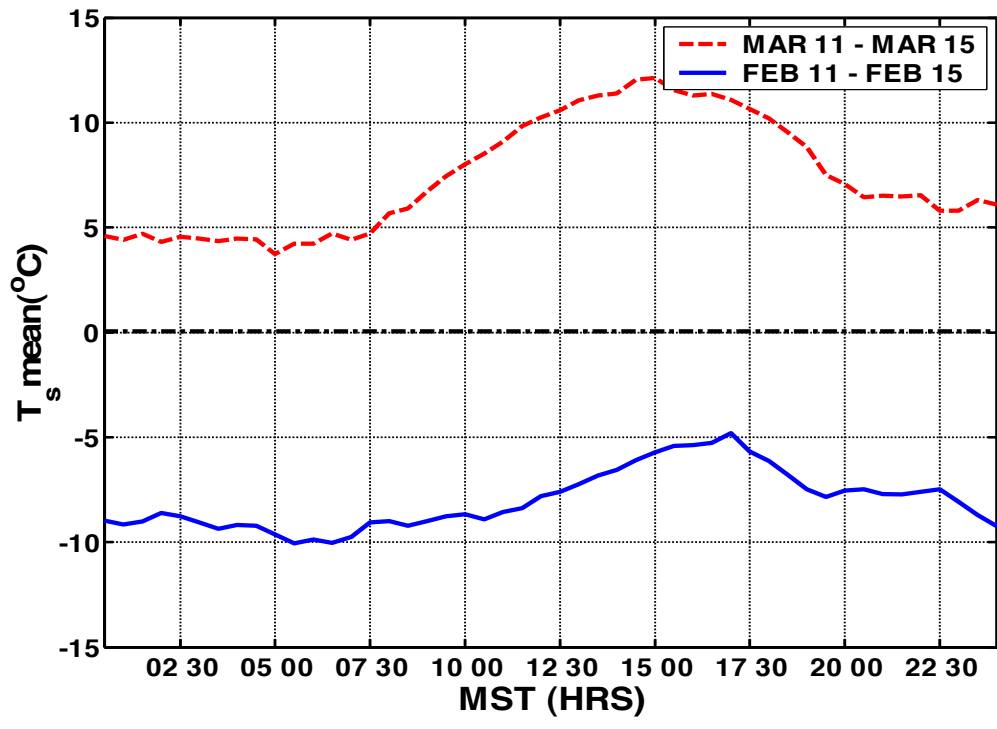


Figure 4.7 5 day ensemble average of mean temperature measured at 9.16 m AGL at Kennecott for February and March 2004.

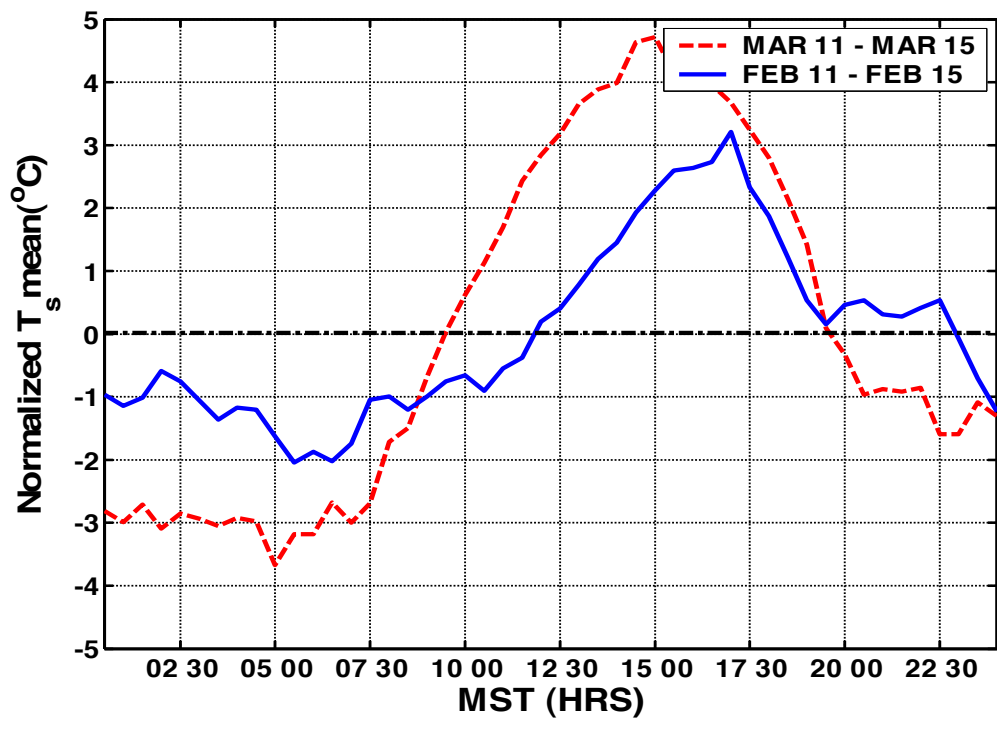


Figure 4.8 5 day ensemble average of normalized mean temperature measured at 9.16 m AGL at Kennecott for February and March 2004.

Nighttime cooling associated with radiation loss from the surface gives rise to a down valley wind system that fills the valley with cold dense air. The stable boundary layer grows over the nighttime suppressing the turbulence and shear stress. Daytime heating of the surface, on the other hand causes the convective boundary layer to grow and the shear stress and turbulence intensity to increase. Figure 4.9 compares the shear stress averaged over the 5 day period of the first persistent inversion episode from 11 through 15 February with the 5 day period from 11 through 15 March that was not in a cold pool. The mean shear stress for February was only 6% of the mean shear stress recorded in March. The movement of the dense cold air is suppressed by the surrounding mountains as a result of which low shear stress is observed during the persistent cold air pool.

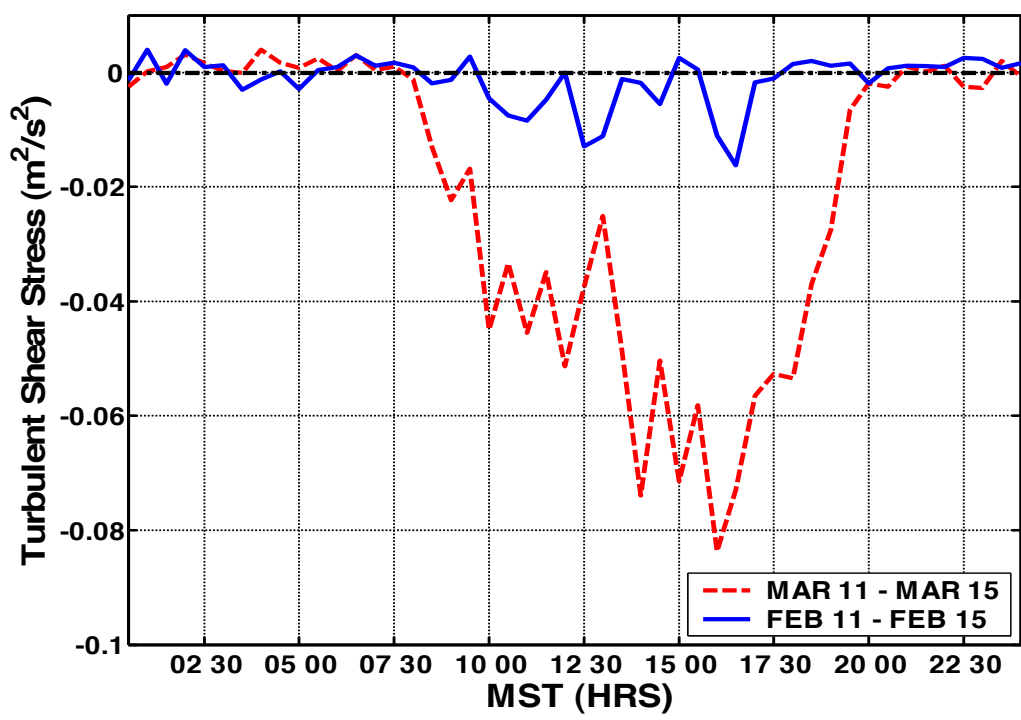


Figure 4.9 Shear stress averaged from 11 through 15 February 2004 and compared to shear stress averaged from 11 through 15 March 2004 at Kennecott.

Figure 4.10 depicts the variation of sensible heat flux during a persistent inversion in February as compared to the sensible heat flux variation during a non cold pool period in March 2004. As explained above, the mountains confine the cold dense air which coupled with the presence of snow and clouds prevents the radiation from the sun to heat the surface and hence very low magnitudes of sensible heat flux are observed during the persistent cold air pool. Also, higher temperature differences between the surface and the air near the surface during nighttime caused higher radiation losses resulting in higher negative sensible heat flux during March when compared to that during the persistent inversion in February. Even though the valley weather for February and March were characterized by clear skies, the average of sensible heat flux during the persistent cold air pool episode in February is only 4% of the average sensible heat flux in March.

Latent heat flux is defined as the flux of latent heat from the surface to the atmosphere associated with evaporation of water at the surface. Latent heat flux is defined as,

$$H_L = L_v * \overline{W'Q'} \text{ (W/m}^2\text{)}$$

where, L_v = Latent heat of vaporization (2.45×10^6 J/kg),

W' = Turbulent fluctuation of velocity in the vertical direction, (m/s)

Q' = Turbulent fluctuations of specific humidity.

The daytime maximum in latent heat flux during March is approximately 4 times the maximum latent heat flux during February (Figure 4.11). Also, the average of latent heat flux during the inversion in February was only 10% of the average latent heat flux during March. Insufficient heating of the surface can be attributed as the reason for low magnitudes of moisture fluxes.

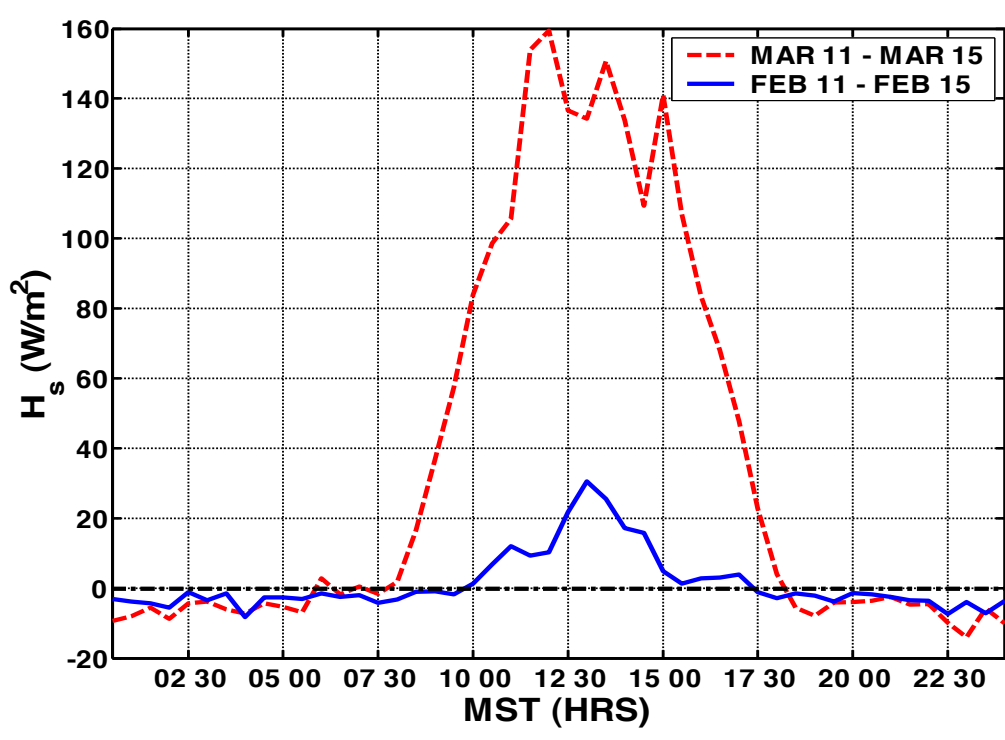


Figure 4.10 Sensible heat flux averaged from 11 through 15 February 2004 and compared to sensible heat flux averaged from 11 through 15 March 2004 at Kennecott.

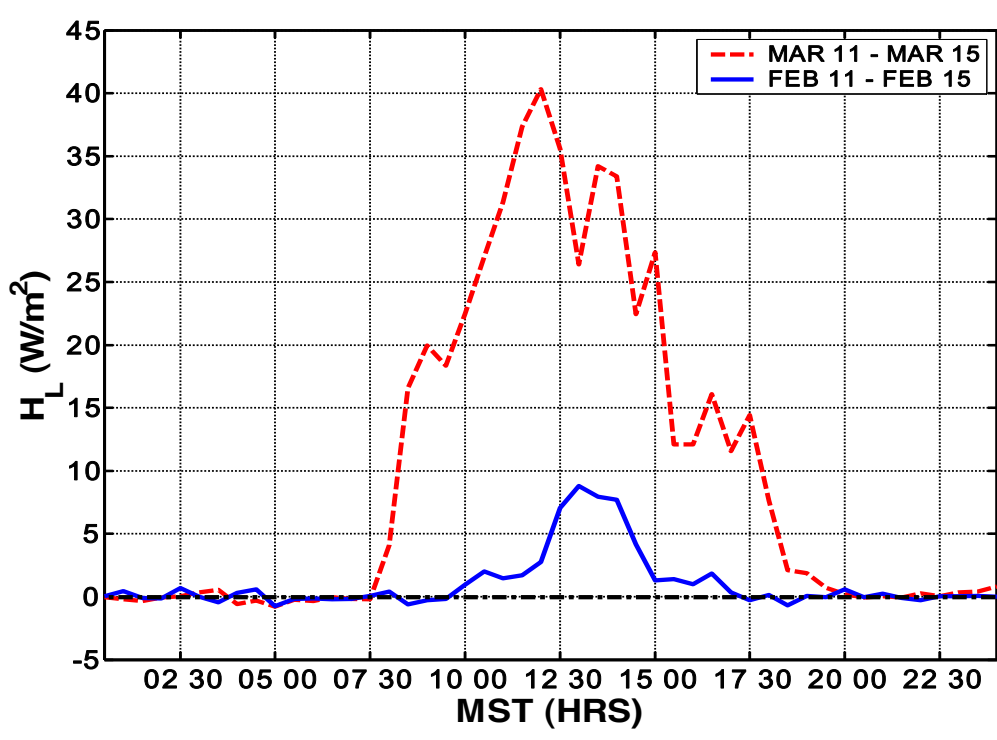


Figure 4.11 Latent heat flux averaged from 11 through 15 February 2004 and compared to latent heat flux averaged from 11 through 15 March 2004 at Kennecott.

Radiation from the sun heats the surface giving rise to thermals that rise in the atmosphere. This process coupled with turbulent momentum flux generates turbulence resulting in an increase in turbulent kinetic energy daytime. Longwave radiative loss at night cools the surface and air displaced vertically by turbulence would experience a buoyancy force pushing it towards its starting height. Low magnitudes of turbulent kinetic energy during nighttime result from stable conditions that tend to suppress or consume the turbulence in the atmosphere. Fig 4.12 depicts the variation of turbulent kinetic energy during the first persistent inversion episode of February 2004 compared to turbulent kinetic energy variation in March 2004. Notice that the turbulent kinetic energy is being suppressed throughout the persistent inversion episode. The average turbulent kinetic energy over the entire persistent inversion episode in February was less than 25% of the turbulent kinetic energy averaged from 11 through 15 March. Figure 4.13 shows the variation of friction velocity at the Kennecott site in February and March 2004. Low friction velocity is an indication of the capability of a persistent inversion episode to suppress and act as sink of turbulence.

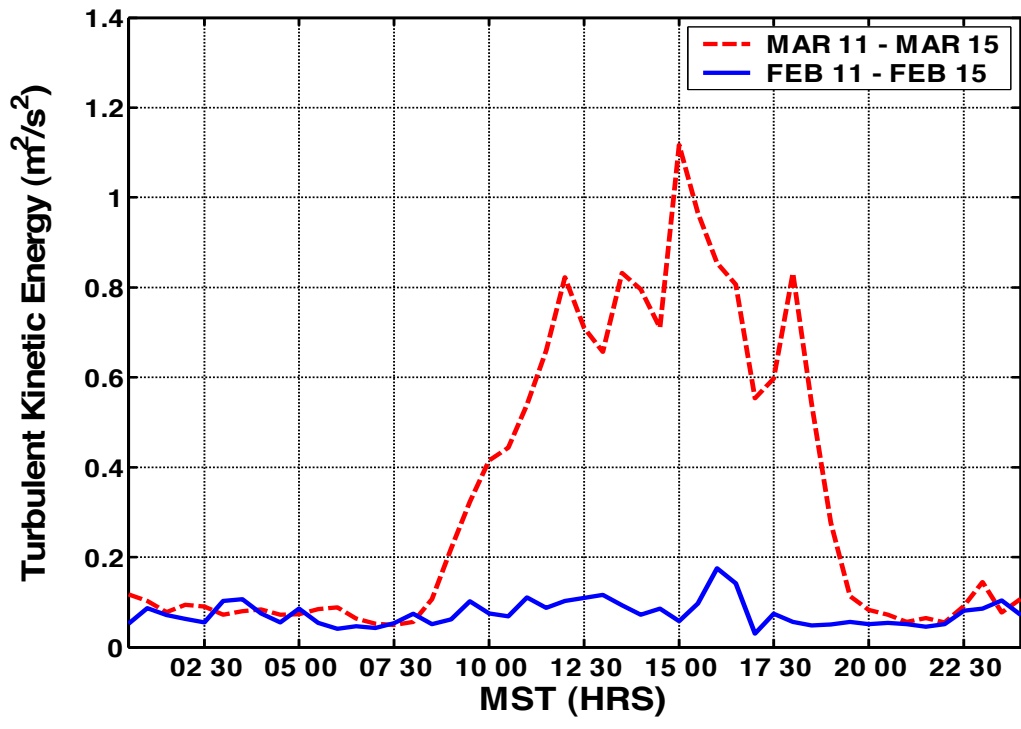


Figure 4.12. TKE averaged from 11 through 15 February 2004 and compared to TKE averaged from 11 through 15 March 2004 at Kenecott.

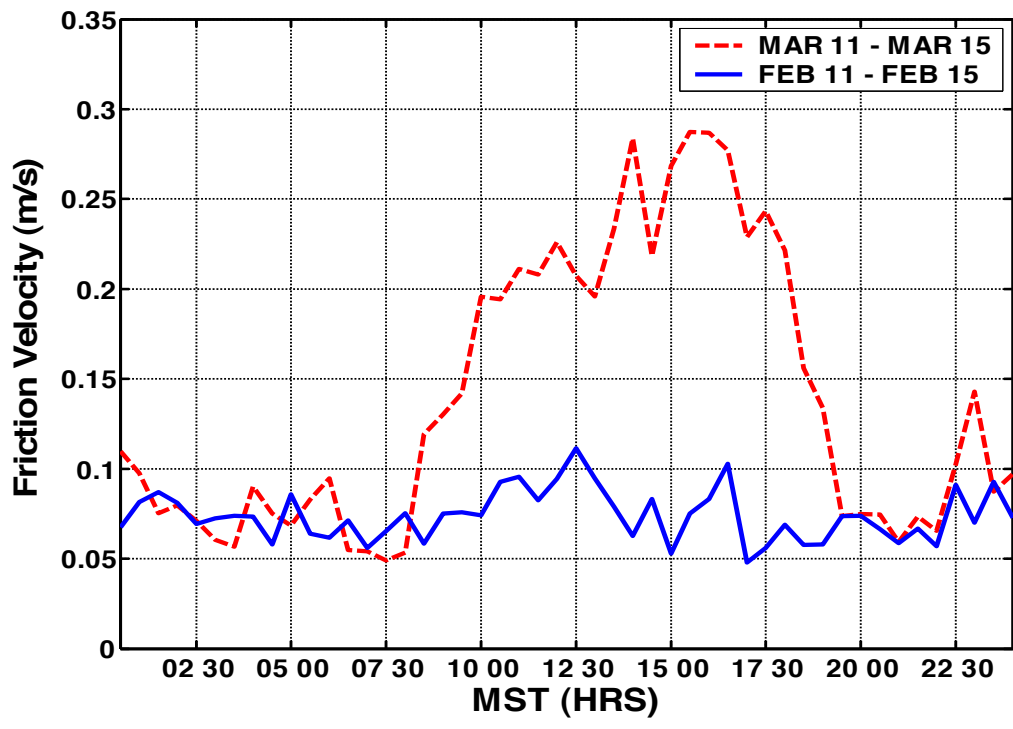


Figure 4.13. Friction velocity averaged from 11 through February 2004 as compared to friction velocity averaged from 11 through 15 March 2004 at Kenecott.

Convective boundary layer growth and down wave mixing of the stronger winds higher in the atmosphere during daytime result in an increase in wind speeds. With no inversion to suppress the convective boundary layer growth, wind speeds in March are greater than wind speeds recorded during the inversion episode in February as seen in Figure 4.14. It is interesting to note that the wind speeds during the inversion episode are greater at night indicating that the nighttime downslope flows are stronger than the daytime upslope flows. Kennecott is located towards the west-south west end of the valley at the foot of Ocquirh mountains. Winds blow from east- south east direction during the day and from west during the night as seen in Figure 4.15. The persistent inversion episode displayed strong westerly or strong down slope flows during the nighttime and weak easterly or upslope flows during daytime. March on the other hand experienced strong easterly or upslope flows with weak westerly or down slope flows during nighttime. Similarity in wind direction between the persistent cold air pool in February and non cold air pool episode in March indicates that upslope and down slope wind system dominated over the up valley and down valley wind system at the Kennecott site.

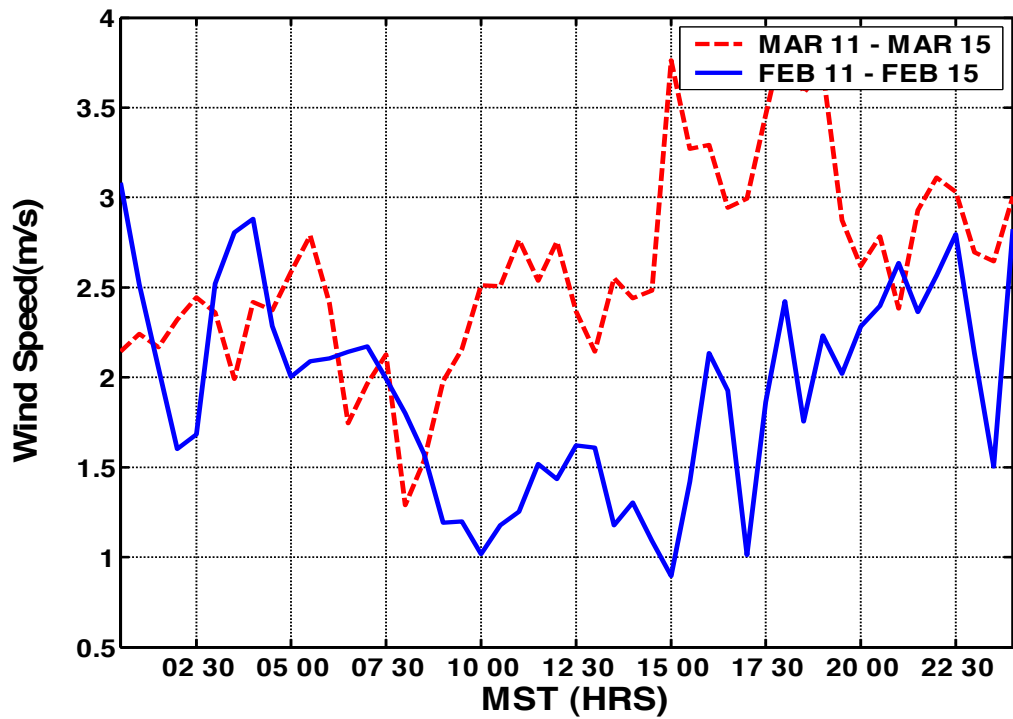


Figure 4.14. Wind speed averaged from 11 through 15 February 2004 and compared to wind speed averaged from 11 through 15 March 2004 at Kennecott.

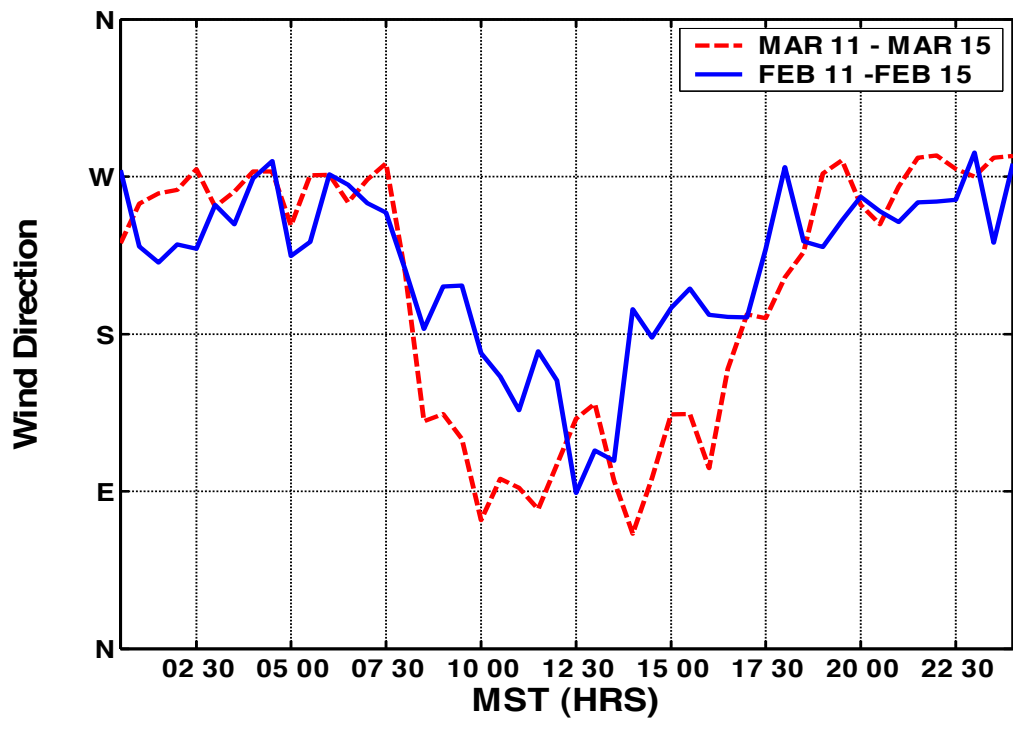


Figure 4.15. Wind direction averaged from 11 through 15 February 2004 and compared to wind direction averaged from 11 through 15 March 2004 at Kennecott.

CHAPTER 5

CONCLUSIONS

February 2004 witnessed two persistent cold air pool episodes separated by a washout event. The first persistent inversion began on 11 February probably from nighttime radiative cooling from the previous day and ended on 15 February. Advection of warm southerly flows began on 16 February and destroyed the first episode by 19 February. Following the washout, the second persistent cold air pool lasted from 20 through 24 February. The valley meteorology during the two inversion episodes was distinctly different from each other. The first episode was characterized by clear skies, good visibility and no precipitation while the second episode consisted of low level clouds, very poor visibility and considerable amount of rain. Even though the valley weather for the two episodes was very different, both episodes displayed transition between two different types of inversion, namely the surface based inversion and a well mixed layer at the surface capped by an elevated inversion. Both episodes displayed the transition from a surface based inversion at night as a result of nighttime cooling and with the daytime heating, the surface based inversion transitioned into a well mixed layer capped by an elevated inversion.

Comparing the micrometeorological variables of heat and momentum fluxes during the first persistent inversion episode in February to a time period in March when there was no inversion revealed that the persistent cold air pools possessed the characteristic of suppressing turbulence. The average turbulent kinetic energy during the persistent inversion was observed to be suppressed by over 70%. Similarly, the average sensible heat flux and momentum flux during the persistent inversion were observed to be only 4% and 6% of the average sensible heat flux and momentum flux recorded in March 2004 respectively. Comparison of wind speeds and wind direction at the Kennecott site for February and March 2004 showed strong up slope and down slope wind system as opposed to up valley and down valley wind system primarily due to the location of the Kennecott site. The down slope winds during the nighttime were stronger than the day time upslope winds during the persistent inversion episode of February 2004. On the contrary, the daytime upslope winds were stronger than the nighttime down slope winds during a non cold air pool episode in March 2004.

APPENDIX



(a)



(b)



(c)



(d)

A.1. Salt Lake Valley on 11 February 2004 from the WBB weather station in University of Utah at (a) 0700 hrs LST, (b) 1000 LST hrs LST, (c) 1300 hrs LST and (d) 1600 hrs LST. Courtesy of MesoWest.



(a)

(b)



(c)

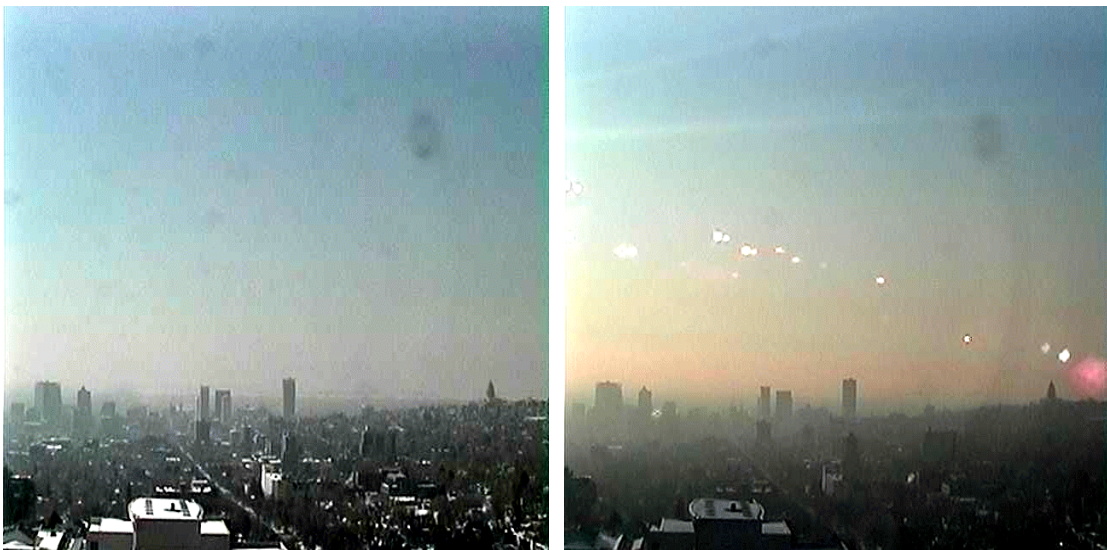
(d)

A.2. Salt Lake Valley on 12 February 2004 from the WBB weather station in University of Utah at (a) 0700 hrs LST, (b) 1000 LST hrs LST, (c) 1300 hrs LST and (d) 1600 hrs LST. Courtesy of MesoWest.



(a)

(b)



(c)

(d)

A.3. Salt Lake Valley on 13 February 2004 from the WBB weather station in University of Utah at (a) 0700 hrs LST, (b) 1000 LST hrs LST, (c) 1300 hrs LST and (d) 1600 hrs LST. Courtesy of MesoWest.



(a)



(b)



(c)



(d)

A.4. Salt Lake Valley on 14 February 2004 from the WBB weather station in University of Utah at (a) 0700 hrs LST, (b) 1000 LST hrs LST, (c) 1300 hrs LST and (d) 1600 hrs LST. Courtesy of MesoWest.



(a)

(b)



(c)

(d)

A.5. Salt Lake Valley on 15 February 2004 from the WBB weather station in University of Utah at (a) 0700 hrs LST, (b) 1000 LST hrs LST, (c) 1300 hrs LST and (d) 1600 hrs LST. Courtesy of MesoWest.



(a)

(b)



(c)

(d)

A.6. Salt Lake Valley on 16 February 2004 from the WBB weather station in University of Utah at (a) 0700 hrs LST, (b) 1000 LST hrs LST, (c) 1300 hrs LST and (d) 1600 hrs LST. Courtesy of MesoWest.



(a)



(b)



(c)



(d)

A.7. Salt Lake Valley on 17 February 2004 from the WBB weather station in University of Utah at (a) 0700 hrs LST, (b) 1000 LST hrs LST, (c) 1300 hrs LST and (d) 1600 hrs LST. Courtesy of MesoWest.



(a)



(b)

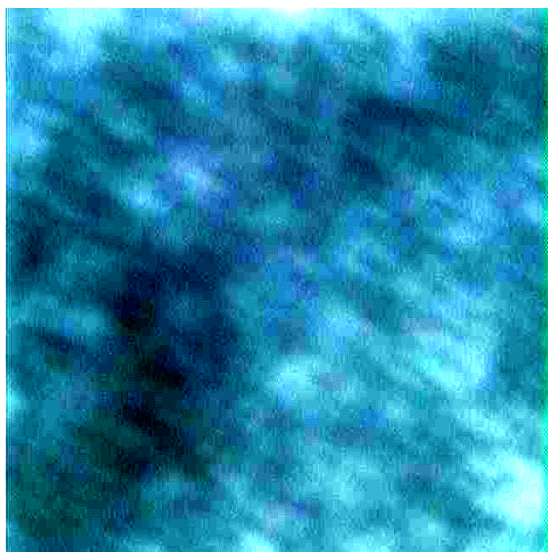


(c)



(d)

A.8. Salt Lake Valley on 18 February 2004 from the WBB weather station in University of Utah at (a) 0700 hrs LST, (b) 1000 LST hrs LST, (c) 1300 hrs LST and (d) 1600 hrs LST. Courtesy of MesoWest.



(a)



(b)



(c)



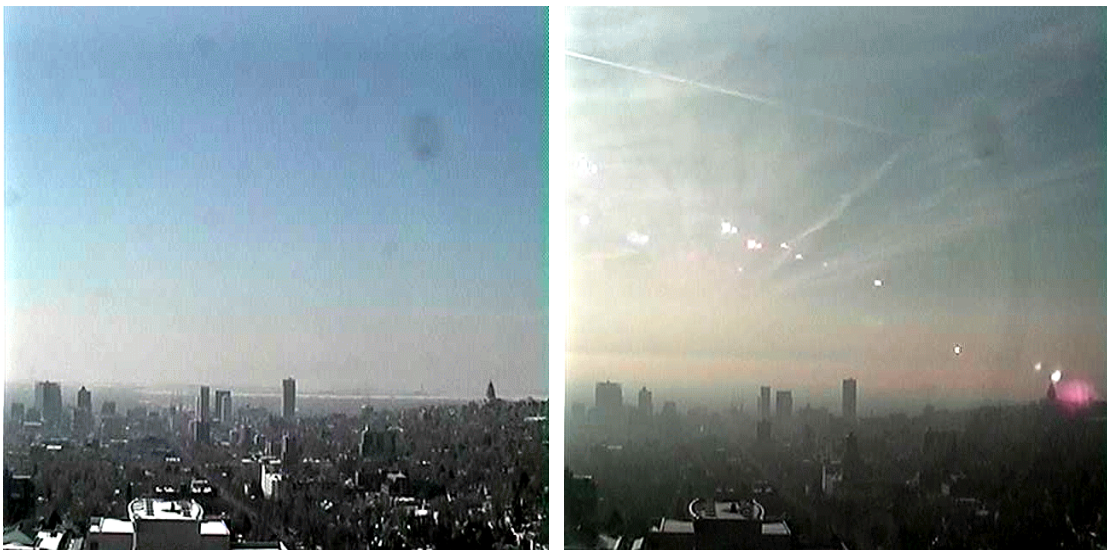
(d)

A.9. Salt Lake Valley on 19 February 2004 from the WBB weather station in University of Utah at (a) 0700 hrs LST, (b) 1000 LST hrs LST, (c) 1300 hrs LST and (d) 1600 hrs LST. Courtesy of MesoWest.



(a)

(b)



(c)

(d)

A.10. Salt Lake Valley on 20 February 2004 from the WBB weather station in University of Utah at (a) 0700 hrs LST, (b) 1000 LST hrs LST, (c) 1300 hrs LST and (d) 1600 hrs LST. Courtesy of MesoWest.



(a)

(b)



(c)

(d)

A.11. Salt Lake Valley on 21 February 2004 from the WBB weather station in University of Utah at (a) 0700 hrs LST, (b) 1000 LST hrs LST, (c) 1300 hrs LST and (d) 1600 hrs LST. Courtesy of MesoWest.



(a)

(b)



(c)

(d)

A.12. Salt Lake Valley on 22 February 2004 from the WBB weather station in University of Utah at (a) 0700 hrs LST, (b) 1000 LST hrs LST, (c) 1300 hrs LST and (d) 1600 hrs LST. Courtesy of MesoWest.



(a)

(b)



(c)

(d)

A.13. Salt Lake Valley on 23 February 2004 from the WBB weather station in University of Utah at (a) 0700 hrs LST, (b) 1000 LST hrs LST, (c) 1300 hrs LST and (d) 1600 hrs LST. Courtesy of MesoWest.



(a)

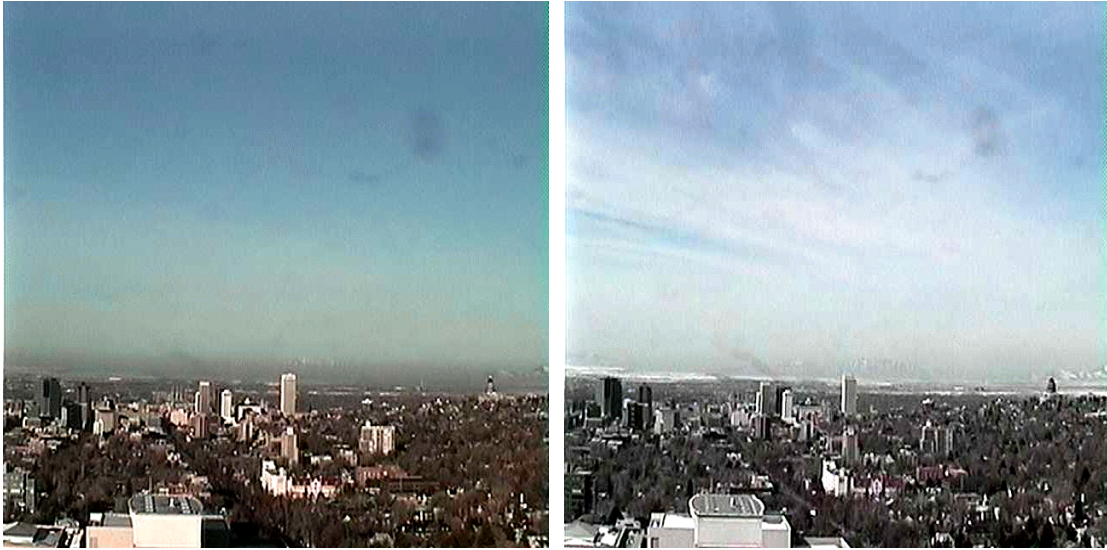
(b)



(c)

(d)

A.14. Salt Lake Valley on 24 February 2004 from the WBB weather station in University of Utah at (a) 0700 hrs LST, (b) 1000 LST hrs LST, (c) 1300 hrs LST and (d) 1600 hrs LST. Courtesy of MesoWest.



(a)

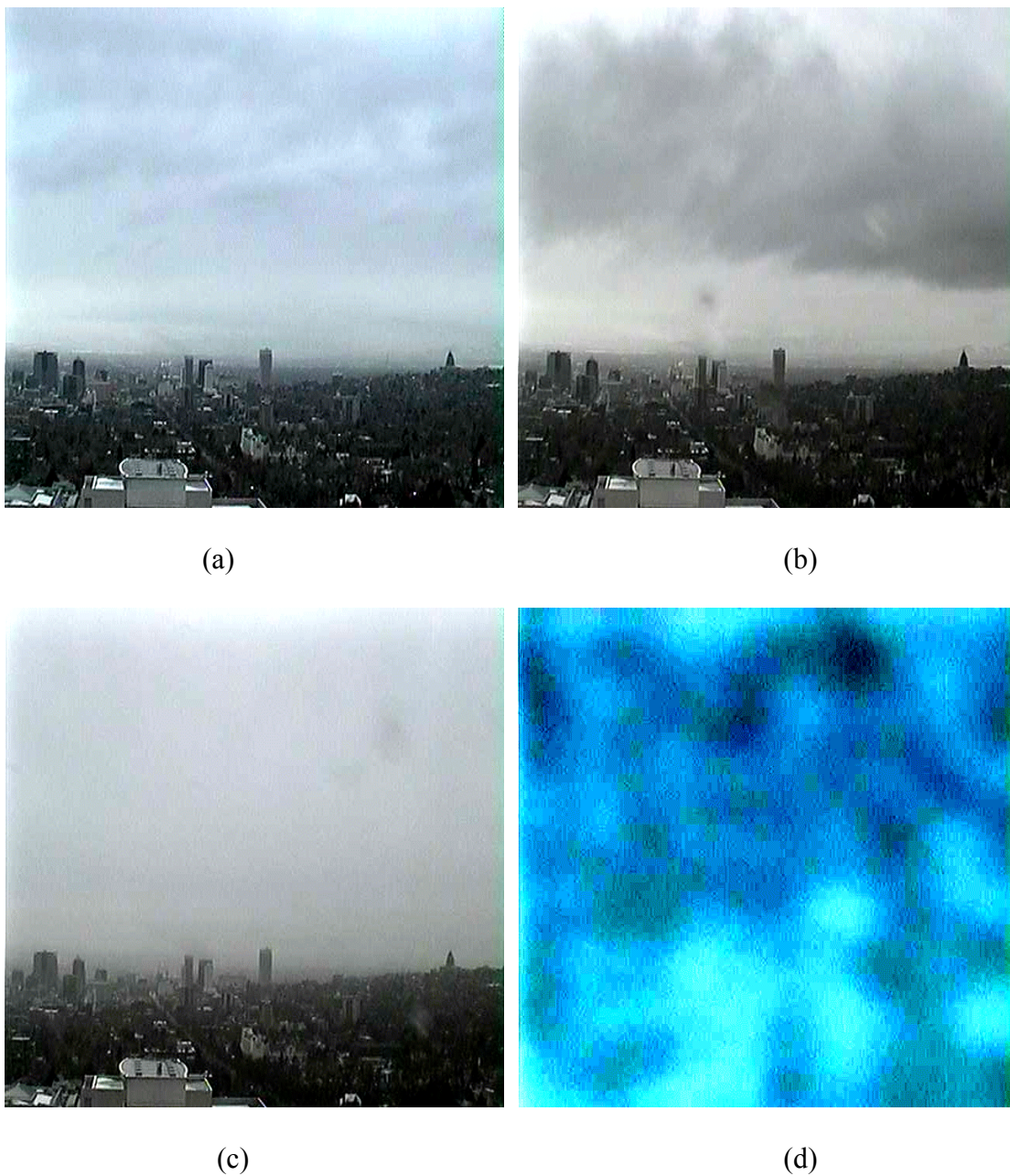
(b)



(c)

(d)

A.15. Salt Lake Valley on 25 February 2004 from the WBB weather station in University of Utah at (a) 0700 hrs LST, (b) 1000 LST hrs LST, (c) 1300 hrs LST and (d) 1600 hrs LST. Courtesy of MesoWest.



A.16. Salt Lake Valley on 26 February 2004 from the WBB weather station in University of Utah at (a) 0700 hrs LST, (b) 1000 LST hrs LST, (c) 1300 hrs LST and (d) 1600 hrs LST. Courtesy of MesoWest.



(a)

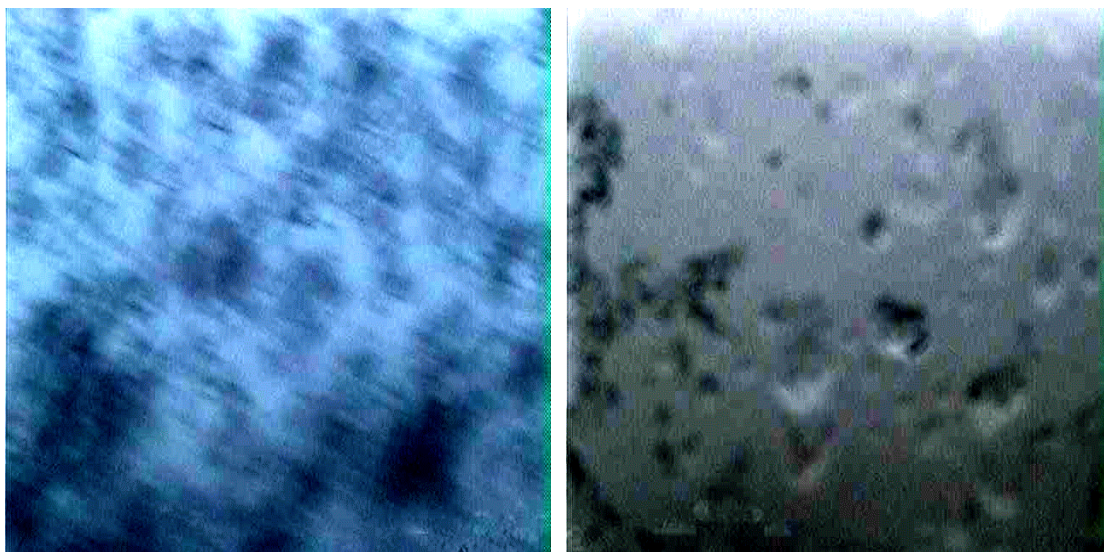
(b)



(c)

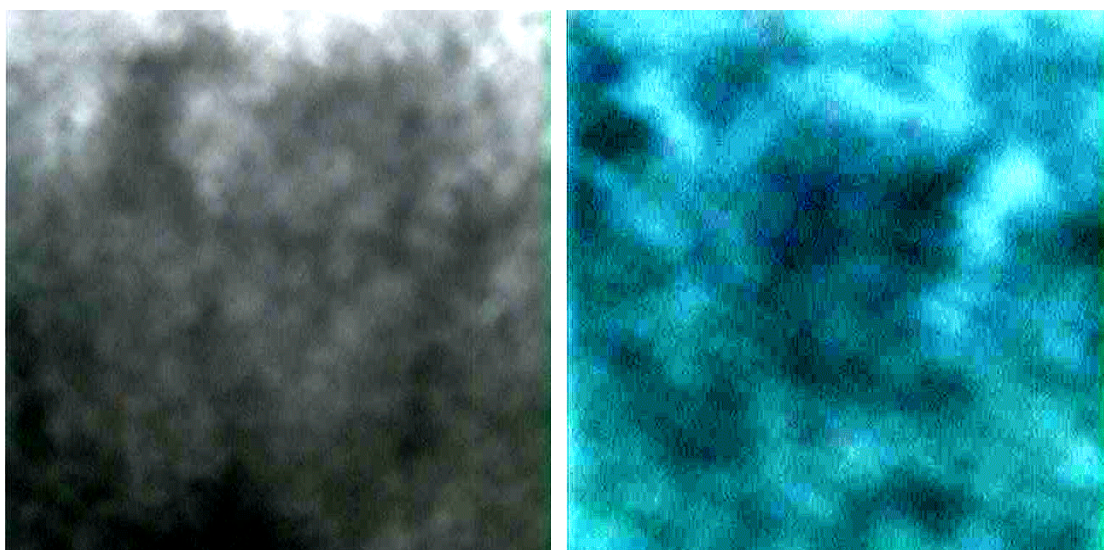
(d)

A.17. Salt Lake Valley on 27 February 2004 from the WBB weather station in University of Utah at (a) 0700 hrs LST, (b) 1000 LST hrs LST, (c) 1300 hrs LST and (d) 1600 hrs LST. Courtesy of MesoWest.



(a)

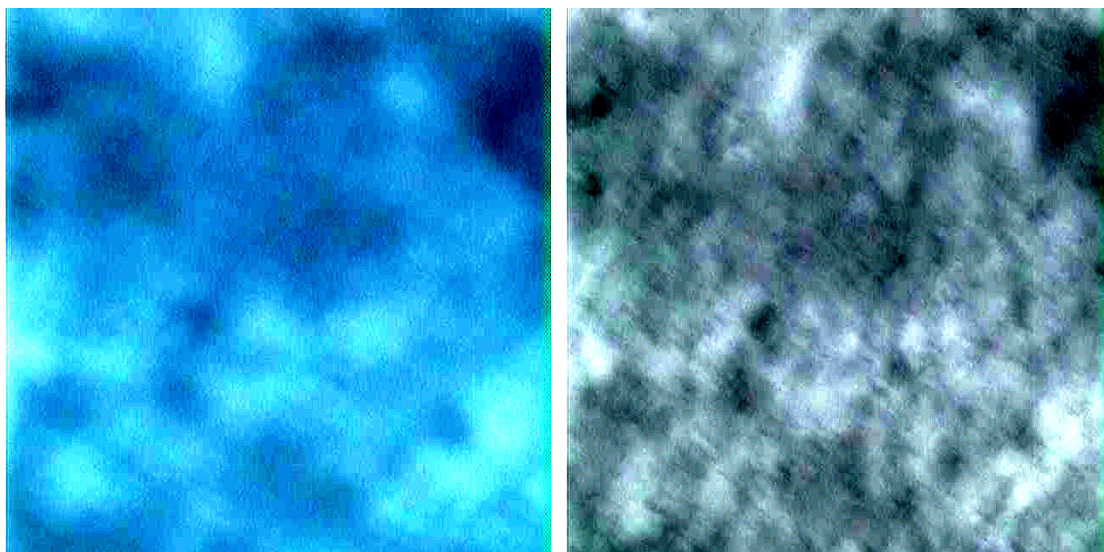
(b)



(c)

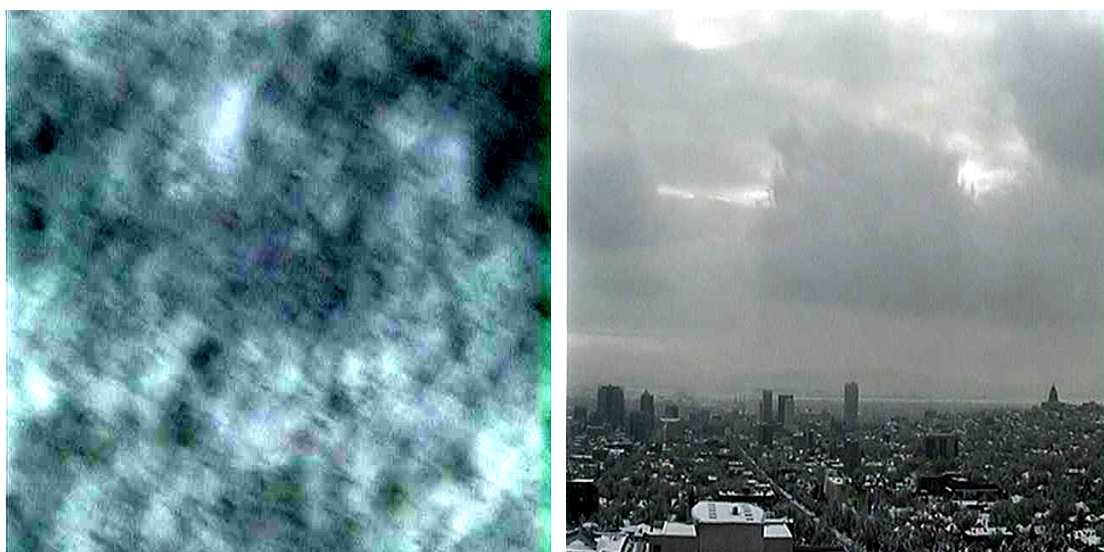
(d)

A.18. Salt Lake Valley on 28 February 2004 from the WBB weather station in University of Utah at (a) 0700 hrs LST, (b) 1000 LST hrs LST, (c) 1300 hrs LST and (d) 1600 hrs LST. Courtesy of MesoWest.



(a)

(b)



(c)

(d)

A.19. Salt Lake Valley on 29 February 2004 from the WBB weather station in University of Utah at (a) 0700 hrs LST, (b) 1000 LST hrs LST, (c) 1300 hrs LST and (d) 1600 hrs LST. Courtesy of MesoWest.

REFERENCES

1. Stephen Holets and Robert N. Swanson, 1981, *Journal of Applied Meteorology*, v20, pgs 890 – 899. TITLE: High-Inversion Fog Episodes in Central California
2. Jeff Johnson, Nov. 21, 2000, Western Region Technical Attachment NO. 00-12. TITLE: Case study of a persistent cold pool in the Helena valley
3. Tsengdar J. Lee, Roger A. Pielke, Robert C. Kessler and John Weaver, 1989, *Monthly Weather Review*, v117, pgs 2041 – 2058. TITLE: Influence of Cold Pools Downstream of Mountain Barriers on Downslope Winds and Flushing
4. W. M. Lockhart, 1943, *Massachusetts Institute of Technology Meteorological Papers*, v1, pgs 11-20. TITLE: A winter fog in the interior, Characteristic weather phenomena of California
5. Zdravko Petkovsek, 1978, *Zetschrift fur Meteorologie*, v28, pgs 333-340. TITLE: Relief Meteorologically Relevant Characteristics of Basins
6. Zdravko Petkovsek, 1980, *Zetschrift fur Meteorologie*, v30, pgs 379-382. TITLE: Additional relief meteorologically relevant characteristics of basins
7. Zdravko Petkovsek, 1992, *Meteorology and Atmospheric Physics*, v47, pgs 237-245. TITLE: Turbulent Dissipation of Cold Air Lake in a Basin
8. P.J. Reddy, D. E. Barbarick and R. D. Osterburg, 1995, *Journal of Applied Meteorology*, v34, pgs. 616- 615. TITLE: Development of a statistical model for forecasting episodes of visibility degradation in the Denver Metropolitan area
9. Ronald Smith, Jan Paegle, Terry Clark, William Cotton, Dale Durran, Gregory Forbes, John Marwitz, Cliff Mass, John McGinley, Hua-lu Pan and Martin Ralph, 1997, *Bulletin of the American Meteorological Society*, v78, pgs. 877-892. TITLE: Local and remote effects of mountain on weather: Research needs and opportunities
10. Roland B. Stull, 1988, “An introduction to boundary layer meteorology”, Kluwer Academic Publishers, Dordrecht, The Netherlands.

11. T. Vrhovec, 1991, *Meteorology and Atmospheric Physics*, v46, pgs. 91-99.
TITLE: A cold air lake formation in a basin – A simulation with a mesoscale numerical model
12. C. D. Whiteman, S. Zhong W. J. Shaw, J. M. Hubbe, X. Bian and J. Mittelstadt, 2001, *Weather and Forecasting*, v16, pgs. 432-447. TITLE: Cold pools in the Columbia Basin
13. C. David Whiteman, Xindi Bian and Shiyuan Zhong, 1999, *Journal of Applied Meteorology*, v38, pgs. 1103-1117. TITLE: Wintertime evolution of the temperature inversion in the Colorado Plateau Basin
14. C. David Whiteman, 1990, "Observations of thermally developed wind systems in mountainous terrain." Chapter 2 in *Atmospheric Processes Over Complex Terrain*, (W. Blumen, Ed.), *Meteor. Monogr.*, v23 (no. 45), American Meteorological Society, Boston, Massachusetts, pages 5-42.
15. James M. Wilczak, Steven P. Oncley and Steven A. Stage, 2001, *Boundary-Layer Meteorology*, v99, pgs 127-150. TITLE: Sonic anemometer tilt correction algorithms
16. Paul G. Wolyn and Thomas B. McKee, 1989, *Monthly Weather Review*, v117, pgs. 461-472. TITLE: Deep stable layers in the Intermountain Western United States
17. Chang-Han Yu and Roger A. Pielke, 1986, *Atmospheric Environment*, v20, pgs. 1751-1762. TITLE: Mesoscale air quality under stagnant synoptic cold season conditions in the Lake Powell area
18. Shiyuan Zhong, C. David Whiteman, Xindi Bian, William J. Shaw and John M. Hubbe, 2001, *Monthly Weather Review*, v129, pgs. 2600-2613. TITLE: Meteorological processes affecting the evolution of a wintertime cold air pool in the Columbia Basin